Role of trait combinations, habitat matrix and network topology in metapopulation recovery from regional extinction

Gimenez Noya, Jose; Robins, Peter; Jenkins, Stuart

Limnology and Oceanography

DOI:
10.1002/lno.11347

Published: 01/04/2020

Peer reviewed version

Role of trait combinations, habitat matrix and network topology in metapopulation recovery from regional extinction

Luis Giménez[1,2] Peter Robins[1] and Stuart Jenkins[1]

1. School of Ocean Sciences, Bangor University, LL59 5AB, Menai Bridge, Isle of Anglesey, United Kingdom.
2. Biologische Anstalt Helgoland, Alfred Wegener Institute, Helmholtz Centre for Polar and Marine Research, 27498 Helgoland, Germany.

Kewwords: connectivity, disturbance, dispersal, eddies, fronts, metapopulation, pelagic larvae

Abstract

We studied the role of oceanographic conditions and life history strategies on recovery after extinction in a metapopulation of marine organisms dispersing as pelagic larvae. We combined an age structured model with scenarios defined by realistic oceanographic conditions and species distribution along the Irish Sea coast (North Europe). Species life history strategies were modelled combining the dispersal behaviours with two levels of fecundity. Recovery times were quantified after simulating extinction in four regions. Two alternative strategies (high fecundity or larval tidal transport) led to short recovery times, irrespective of the effects of other drivers. Other strategies and low larval survival exacerbated the effects of oceanographic conditions on recovery times: longer times were associated with for example the presence of frontal zones isolating regions of extinction. Recovery times were well explained by the connectivity of each focal population with those located outside the area of extinction (which was higher in the so-called small world topologies), but not by subsidies (direct connections with populations located nearby). Our work highlights the complexities involved in population recovery: specific trait combinations may blur the effects of the habitat matrix on recovery times; k-strategists (i.e. with low fecundities) may achieve quick recovery if they possess the appropriate dispersal traits. High larval mortality can exacerbate the effect of oceanographic conditions and lead to heterogeneity in recovery times. Overall, processes driving whole network topologies rather than conditions surrounding local populations are the key to understand patterns of recovery.

INTRODUCTION

Disturbance is a fundamentally important process in all ecological systems, modifying resource availability and causing disruption to population, community or ecosystem structure (White and Pickett 1985). A disturbance event by definition occurs over a relatively discrete period of time, but the spatial scale over which it operates can vary from that of an individual through to whole ecosystems. For instance, in the marine environment regional scale disturbances covering areas of the order of 10-10^3 km may be produced by a range of drivers including summer anoxia at the sea bed (Bishop et al. 2006, Dias and Rosenberg 2008), storms (Woodley et al. 1981), heat waves, extreme temperatures (Glynn 1993, Coma et al. 2009) and pathogens (Miller and Colodey 1983, Lessios 2016). Many disturbance regimes are currently changing, with profound shifts expected in the coming decades as the consequence of climate change and increasing encroachment of human activity over previously pristine habitats (Turner 2010). Current climate change projections, for example, suggest that extreme weather events, including heat waves and storms are likely to increase in frequency and magnitude (e.g. Burrows et al. 2014, Di Lorenzo and Mantua 2016) leading to regional scale levels of mass mortality. Current coral bleaching as the consequence of the recent El Nino is an example of the spread and importance of regional scale events (Tollefson 2016).

For marine species, determining the fate of pelagic larvae is central to understanding the consequences of mass mortalities in terms of population recovery. Benthic or demersal populations are patchily distributed, often in association with specific habitats, but populations are connected through a dispersive larval stage (Cowen and Spounagle 2009). It is therefore appropriate to use the concept of metapopulation, for such populations. Metapopulation theory was developed with the idea of modelling local extinction and recovery in populations with

limited connectivity and has provided valuable theoretical framework for conservation ecology (Hanski and Gaggiotti 2004), but the concept has been expanded to consider cases where populations are well connected. Hence one may define marine metapopulations as set of local populations of adults connected through larval dispersal (Arsmworth 2002) with the direction and magnitude of larval dispersal pathways determining patterns of connectivity and hence the extent to which different locations receive larval subsidies (Levin 2006, Cowen and Sponaugle 2009).

Given the major logistical challenges of directly quantifying larval connectivity, most effort has focused on modelling patterns of larval transport through hydrodynamic models (e.g. Cowen et al. 2006, Paris et al. 2007, Ayata et al. 2010, Robins et al. 2013). In such models, the connectivity and retention coefficients represent the main characteristic of the habitat matrix (i.e. the habitat through which organisms disperse and migrate: Wiens 1997, Joly et al. 2001, Shima and Swearer 2009). These models highlight the importance of local hydrodynamic conditions and species-specific larval behaviours in driving population persistence (e.g. Cowen et al 2006, North et al. 2008, Botsford et al. 2009); hence, they should also drive the rate of recovery from extinction. A critical output of such models is that in situations where the model domain covers sufficiently large spatial scales (e.g. Cowen et al. 2006, Robins et al. 2013) limitations in dispersal define regions that are weakly connected with each other. Such spatial patterns may result in a reduced capacity to recover from mass mortalities if the scale of disturbance matches the scale of connectivity.

Models coupling dispersal with local processes have helped to understand the conditions of persistence of populations (Armsworth 2002, Hastings and Botsford 2006, Artzy-Randrup and Stone 2010). Such work has recognised pressures on local populations but given the increasing

regional scale of disturbance events there is in addition an urgent need to understand the drivers of recovery from regional extinction. Marine metapopulation models should help us to understand *how quickly* local populations may recover from mass mortalities especially if they are applied to realistic metapopulations. Here, we applied an age structured metapopulation model to a realistic scenario by modelling the dynamics of a coastal species distributed in fragmented populations in the Irish Sea (Northwest Europe). The Irish Sea, like many other coastal areas worldwide, is impacted by regional and global scale phenomena (see Robins et al. 2016) exposed to a range of anthropogenic stressors leading to local and regional mortality events of benthic species (e.g. Malham et al. 2012). Here, we develop a metapopulation model for coastal species restricted to sheltered bays and estuaries (habitat patches) in order to examine patterns of recovery from extinction in well-defined regions throughout the Irish Sea. The following questions were addressed: Given an event of regional extinction: (1) Do specific life histories (i.e. a combination of traits such as fecundity and larval behaviour) enhance recovery? In particular, is there any optimal strategy enhancing recovery or are strategies context-dependent, i.e., do they depend on the region within the habitat matrix? (2) What is the role of the habitat matrix in setting the time scale of recovery? More specifically, would larval survival and variations in oceanographic conditions (as captured by the connectivity matrix) lead to significant spatial or temporal patterns in recovery? (3) What is the importance of the network topology? In particular, is recovery explained by retention or direct subsidy to a focal population or is it driven by whole network connectivity to populations located outside the region of extinction?

METHODS

General procedure

We constructed a metapopulation model of a species occupying shallow, sheltered habitats in 40 populations throughout the Irish Sea and dispersing during the larval stage. Specifically, we consider a model species living up to five years and starting to reproduce after the first year of life. The direction and magnitude of connection among discrete populations is given by larval transport matrices, accounting for the physical transport of larvae. The larval transport matrices were modelled based on particle tracking models incorporating realistic three-dimensional hydrodynamic conditions. Three main larval strategies were considered (Robins et al 2013): (1) passive transport (no vertical migration); (2) diel vertical migration (upward swimming during the night and downward swimming during the day); (3) flood tidal migration (upward swimming during the flood phase and downward swimming during the ebb). Vertical swimming speed was set to 3×10^{-3} m s^{-1}, representing ciliated larvae (Chia et al. 1984). Robins et al (2013) showed that dispersal distance, retention or connectivity did not vary in the range of speeds $1\text{-}5 \cdot 10^{-3}$ m s^{-1} but that speeds $<1\text{-}5 \cdot 10^{-3}$ m s^{-1} such patterns would resemble those obtained for passive transport.

Regional extinction events were simulated based on total loss of populations in one of four regions (Fig. 1). Overall, we ran 96 simulations differing in the combination of larval strategy (three levels), combinations of fecundity and larval mortality (two levels, controlled through a composite parameter, see below), timing of larval release (two levels-spring and summer), region of extinction (four regions) and the strength of density-dependent mortality in the benthic phase. For each simulation, the model was run for 200 cycles (= years) followed by an event of regional

extinction. Recovery time was then quantified after running the model for an additional 400 years. The model was run in Matlab^{R} (see Appendix S1 for code).

Metapopulation model and dispersal matrices

The model is a modification of the one developed by Armsworth (2002). Using five age classes and 40 populations the model is as follows:

$$\begin{bmatrix} N(t+1)_1 \\ N(t+1)_2 \\ \vdots \\ N(t+1)_{200} \end{bmatrix} = \begin{bmatrix} M_1 & Q_{1,2} & \cdots & Q_{1,40} \\ Q_{2,1} & M_2 & & Q_{2,40} \\ \vdots & & \ddots & \vdots \\ Q_{40,1} & \cdots 0 & Q_{40,39} & M_{40} \end{bmatrix} \begin{bmatrix} N(t)_1 \\ N(t)_2 \\ \vdots \\ N(t)_{200} \end{bmatrix} \quad (1)$$

There are a total of 40 local matrices (M) corresponding to the populations; each local matrix is based on an age-dependent matrix model:

$$M = \begin{bmatrix} 0 & f\eta l_{p\to p}\sigma & \cdots & f\eta l_{p\to p}\sigma \\ g_1 & 0 & & 0 \\ \vdots & \ddots & & \vdots \\ 0 & \cdots 0 & g_4 & 0 \end{bmatrix} \quad (2)$$

In (2) f is the fecundity, η is the larval survival during pelagic dispersal (i.e. due to sources other than over-dispersion, e.g. predation, stress, food limitation), $l_{p\leftarrow p}$ is the fraction of larvae that would return to the original population if mortality were zero and σ is the probability of settled individuals reaching the first year of age. Notice that we separate physical transport from larval mortality; hence, larval dispersal would be given by $\eta \times l_{p\leftarrow p}$ (or $\eta \times l_{i\leftarrow j}$ see below). In addition, connectivity will be given by $\sigma \times \eta \times l_{p\leftarrow p}$ ($\sigma \times \eta \times l_{i\leftarrow j}$: see e.g. Lett et al. 2015). Here for simplicity, we refer to $l_{p\leftarrow p}$ and $l_{i\leftarrow j}$ as *larval* retention and *larval* connectivity respectively. In equation 1, a series of Q matrices (see equation 3) define the number of larvae originating in

each population that settle and survive over the first year in the local population. Each Q matrix is a square matrix of 5×5 cells (corresponding to the age classes) given by equation 3.

$$Q = \begin{bmatrix} a_{1,1} & a_{1,2} & \cdots & a_{1,5} \\ 0 & 0 & & 0 \\ \vdots & & \ddots & \vdots \\ 0 & \cdots 0 & 0 & 0 \end{bmatrix} \quad (3)$$

For the upper row, $a_{ij} = \sigma \times l_{i \leftarrow j} \times \eta \times f$ represents the product of the larval production and survival, the larval connectivity coefficient ($l_{j \leftarrow i}$).

The larval connectivity and retention coefficients were those given by Robins et al. (2013). Robins et al (2013) used a coupled 3D hydrodynamic and Lagrangian particle tracking model to simulate scenarios where larvae are released at one time in the year and allowed to disperse for 28 days under realistic wind, temperature, tidal and photoperiod conditions. Importantly, the connectivity and retention coefficients were obtained from realistic distribution of populations throughout the region, coastal geography and sea bottom topography, all contributing to the patterns of dispersal.

The number of larvae competent to settle at the end of the pelagic period is a function of the number produced (fecundity rate) and the number of these which survive (mortality rate). We lack any evidence to realistically vary either production or loss of larvae across geographic locations and age class of adult. Hence, fecundity and larval survival rates were modelled as density-independent and constant over the whole model domain and were combined to form a single parameter, $\omega = f \times \eta$; ω may be interpreted as a component of the maternal fitness, i.e. the product of offspring number and survival. Variation in larval survival has been shown to modify patterns of connectivity (Paris et al. 2007); hence, the metapopulation model was run using two values of ω (10 and 10,000 larvae per reproductive adult). The values of ω are chosen in first

instance to cover a wide range in the parameter space. Second, such values cover the range of fecundities and known mortality rates observed in marine invertebrates. For instance, instantaneous daily mortality rates for marine larvae range from 0.22 (Rumrill 1990) to 0.14 (White et al. 2014), resulting in ca. 0.13% to 1.50% survival over 28 days (used to model the connectivity matrices). Combining these estimates ($\eta = 1.3 \times 10^{-3}$ - 1.5×10^{-2}) with the values of the term ω used in the model (10, 10^4), we obtain a realistic range of fecundities (from $f = 10^3$ for ω = 10 to $f = 10^7$ for $\omega = 10^4$).

Overall, the model incorporates two sources of mortality, one that was captured in the parameter η, and one that was caused by dispersal away from suitable habitat (subsequently termed overdispersion). Overdispersion is reflected in the coefficients of connectivity and retention since at the end of the simulation any larvae that do not reach the population from which they arose or reach one of the other 39 populations are considered dead. Overdispersion is affected by larval behaviour and by temporal changes in oceanographic conditions (Robins et al. 2013). In the present models, we assume that overdispersion and η do not covary, but we recognise potential sources of co-variation; for instance, diel vertical migration may lead to specific patterns of overdispersion while minimising mortality by predation.

The number of larvae arriving to a focal population p, ($S_{t,\, j=p}$) is defined by the contribution of the focal population, accounted for in the first row of the M matrix (equation 2), and the subsidy from other populations, accounted for in the first row of the Q matrices (equation 3). These contributions are calculated as:

$$S_{t,j=p} = \sum_{k=1}^{5} N_{t,k,j=p} \cdot \omega \cdot l_{p \to p} + \sum_{k=1}^{5} \sum_{j \neq p} N_{t,k,j} \cdot \omega \cdot l_{j \to p} \quad (4)$$

The first term in the right hand side of equation (4) defines the total number of individuals retained as the product of the number of adults, fecundity and survival (= ω), and the larval retention coefficient. The second term defines the input of larvae from other populations (subsequently termed subsidy), similar to retention, but based on the larval connectivity coefficients between each particular population, *j*, and the focal population, *p*. For simplicity, we assume that larval retention or connectivity coefficients are constant across ages and through each event of larval release (no *t* or *k* subscripts in eq. 4). Note that when the focal population, *p,* goes extinct, recovery is in the first instance governed by the subsidy and hence the first term of equation 4 is zero. Eventually, once individuals reach the reproductive age, recovery will also depend on retention coefficients.

Following larval settlement, and over the first year of benthic life, the survival rate, *s*, in the M and Q matrices, was modelled as a density-dependent process according to the Beverton-Holt equation. The number of individuals surviving the first year of life (N_1) was:

$$N_{1,t+1} = \frac{\alpha_0 \cdot S_t}{1+\beta_0 \cdot S_t} \quad (5)$$

Where S_t is the number of larvae arriving to the nursery habitat (eq. 5) and α and β are parameters; the subscript *0* indicates that these correspond to young of the year. We defined α as the density-independent survival parameter (since $N_1/S \rightarrow \alpha$ when $S \rightarrow 0$); β is the density-dependent parameter (if $\beta = 0$, N_1 is proportional to S_t).

In the following years, all individuals experience mortalities depending on the *total* number of individuals present in that habitat. The survival rate in the adult habitat (g_i in the M matrix) was also modelled by a Beverton-Holt equation. Therefore, the number of individuals of age k surviving to the age k+1 is:

212 $$N_{k+1,t+1} = \frac{\alpha_a \cdot N_k}{1+\beta_a \cdot \sum_k N_k} \quad (6)$$

213 where the subscript "a" indicates that the parameters of the function that correspond to the
214 survival of individuals of one or more years of age. The density-dependent coefficient β for both
215 the first year of life, and subsequent years, was varied between 0.1 and 0.0001 to explore the role
216 of benthic survival on recovery. For simplicity, we assume that for all populations $\alpha_0=\alpha_1=1$,
217 $\beta_0=\beta_1=\beta$ in eqs. 4 and 5. In such a model, for each individual simulation, the variation in the
218 response variables among populations depended solely on the coefficients of the connectivity
219 matrix. Taken together, the simplifications of α_1, β and ω would result in a "stage-structured"
220 model composed of a juvenile stage (with zero fecundity and one year duration), and an adult
221 stage (with non-zero fecundity and four year duration). However, we prefer to present the model
222 in an "age structured" form shown in eq 1-3 because it is easier to interpret each iteration as
223 equivalent to one year of duration.

224 **Simulations of extinction**

225 Initially the model was run for 200 years, covering 24 different scenarios, varying in all possible
226 combinations of larval strategy (diel, tidal, passive), season (spring, summer), the term ω (=10 or
227 1000 larvae per reproductive adult) and density-dependent coefficient β (=0.1 or 0.0001). Each
228 model simulation was initialized with 10 individuals per age class at each population. In each
229 cycle, the model computed, at time *t*, the number of larvae produced and settled at each site,
230 using equation 3. The number of settlers was then used, also at the time *t*, to update S_t in equation
231 4. Then, the model computed, at the time *t+1*, the number of individuals surviving the first year
232 of life according to equation 5. The number of "first years" was then used to update the term N_k
233 in equation 6, which is used to compute, at the time *t+2*, the number of individuals surviving to

age = 2 years. At a given year $t+i$, the terms in the local matrix (eq. 2) depending on eqs. 4-6 were updated simultaneously according to S_t and the total number of individuals in the adult habitat.

After the initial 200 year run of each of the 24 simulations, we then simulated extinction and measured recovery for four regions: (1) Cardigan Bay (populations 4 to 8 in Fig. 1), (2) Anglesey (populations 9 to 12), (3) Liverpool Bay (populations 13 to 22), and (4) central Ireland (populations 33 to 37). Each extinction and recovery simulation was run separately for each of the four regions, giving a total of 96 simulations (=24×4; i.e. only one region suffered an extinction event at any one time, in a given simulation). We did not simulate extinction in any population located at the border of the model domain since the recovery of such populations should be affected by subsidy populations outside the model domain. Extinction was simulated by setting abundance to zero for all age classes of the populations in the target 'extinction' region. The model was then run for a further 400 "years" and the rate of recovery quantified as T_{50}, the time (in years) required by populations to reach 50% of the asymptotic population size. We run a series of preliminary simulations in order to check the behaviour of the model: these results are detailed in Appendix S2.

Statistical analysis

We used a statistical approach to quantify the average effect of each driver (region of extinction, month of larval release, β and ω) on recovery time (T_{50}). We also studied the time needed for a population to double its size when rare (Appendix 2, Secction 2.2.) but found that T_{50} was more useful as a descriptor of the recovery rates Statistical analyses (on T_{50}) were run in R (R core team 2013). We followed the recommendations of White et al (2014) and focused on effect sizes,

since applying significance testing to simulation outputs would not be appropriate in a modelling exercise. Effect sizes were quantified using two techniques, boosted regression trees (James et al. 2013) and general least squares models (GLS: Zuur et al. 2009, Galecki and Burzykowski 2013); such techniques have been used to identify key drivers of metapopulation connectivity (Treml et al. 2015).

Boosted regression trees (BRT) were carried out following Elith et al. (2008). BRT is a technique of non-linear model fitting based on so called "decision trees". Decision trees partition the predictor space (defined here by our drivers of connectivity) into regions of similar values of the response variable (recovery time) and then fit a constant to each region (Elith et al. 2008). Boosting is a numerical optimization technique minimising the error through the cumulative fitting of additional trees to the data (each tree is fitted to the residuals obtaining from the fit of a previous tree). We use BRT as way to quantify the importance of each predictor, given as their relative influence (i.e. the proportion of the number of trees where a given predictor is fitted). BRT were fitted in R, using the package *dismo* and the function *gbm.step*; this function enables the use of a cross-validation method, based on testing the models of the fraction of the data ("bag fraction" = 0.5 in our case) in order to select optimal number of trees for the model. We fitted four models differing in the "learning rate" (range 0.05 to 0.0005), a parameter controlling the contribution of each tree to the model. All models were fitted with normal residuals and a tree complexity of 5, i.e., considering the highest (five-way) interaction. All model fits led to similar patterns in the relative influence of the predictors on the recovery time; we present the results corresponding to a learning rate of 0.01.

In order to interpret the output of the BRT we present plots of averaged recovery rate in response to all combination of parameters as well as plots of parameter estimates obtained from a general

least square model (GLS). The GLS was fitted using the package *nlme* (Pinheiro and Bates, 2000) considering variance heterogeneity (VarIdent constructor function) and correlations among sites (CorCompSymm function). Although our design was fully replicated, our attempts at fitting the full model for the variance structure led to situations of non-convergence; when this occurred, we reduced the complexity of the variance structure in the starting model. Models were fit using restricted maximum likelihood method (REML).The GLS technique was applied to the logarithmically transformed values of the recovery time. The full model was a 5^{th} order full factorial for both the variance and the fixed structure (i.e. for the fixed structure: $T_{50} \sim \omega$ x β x strategy x month x region) and parameter estimates were extracted.

Network topology

In a separate group of models, we evaluated the role of network topology. First, we evaluated how well recovery time was predicted by local subsidy and retention. In this case we used the coefficient of determination (R^2) as a metric of effect sizes because our focus was on the importance of subsidy or retention in explaining variation in recovery time. Subsidy was defined as the sum of the connectivity coefficients indicating input of larvae towards a focal population. Note that subsidy is calculated as the *sum* of transport coefficients *directly* connecting the focal population to others many of which that may be *inside* the area of extinction. For instance, for a focal population located in the centre of the area of extinction the most likely scenario is that subsidy is entirely dependent on adjacent populations located inside the area of extinction. Larval connectivity to the outside source may occur *indirectly*, i.e. through one or more local populations (e.g. in a stepping stone pattern); it will depend on transport coefficients linking the focal and other populations with those *outside* the area of extinction and it is calculated as a *product*. Hence, for each focal population we used two different indices of connectivity to the

sources located outside the region of extinction, the total connectivity (*CT*) and the one provided by the path giving the maximum connectivity (*CM*). *CT* was defined as the sum of the connections to the populations located outside the region of extinction either direct or indirect (the latter is calculated as a product of coefficients).

$$CT_p = \sum_v (\prod_j l_{ij}^v) \quad (7)$$

In equation (7), each l^v_{ij} is a larval transport coefficient between populations forming a path *v* between the focal population and the source populations located outside the region of extinction. For CT, all paths are considered; one such path, the one used to calculate *CM*, has the maximum product of the associated transport coefficients:

$$CM_p = Max(\prod_j l_{ij}^v) \quad (8)$$

For example, if populations were connected to a source S_0 through a single path (a stepping stone pattern): $S_0 \rightarrow P_1 \rightarrow P_2 \rightarrow P_3$ and larval connectivity were $l_1 \leftarrow_0 = 10^{-1}$, $l_2 \leftarrow_1 = 10^{-1}$, $l_3 \leftarrow_2 = 10^{-2}$ respectively, then $CM_1 = 10^{-1}$, $CM_2 = 10^{-2}$ and $CM_3 = 10^{-4}$. If by contrast S_0 were also connected to P_2 with $l_2 \leftarrow_0 = 10^{-1}$ then $CM_1 = 10^{-1}$, $CM_2 = 10^{-1}$ and $CM_3 = 10^{-3}$, because such alternative path leads to higher *CM* for populations 2 and 3. In many cases, transport, between populations *i* and *j* is bi-directional because of non-zero coefficients occurring in both directions ($lj \leftarrow i > 0$ and $li \leftarrow j > 0$). Bidirectionality in transport between populations is common although in most cases there are strong asymmetries because currents flow in a predominant direction. Where transport between two populations was more symmetrical (i.e. where differences in coefficients were not large) the calculation of CM is based in the first instance on connections with populations from that region, and in the second instance, on the largest coefficient connecting two populations. For example, if we have $S_0 \rightarrow P_1 \rightarrow P_2 \leftrightarrow P_3$ and $l_3 \leftarrow_2 < l_2 \leftarrow_3$ then, for P_2, $l_3 \leftarrow_2$ would still be the appropriate

coefficient because $l_{2\leftarrow 3}$ would only enable subsidy from S_0 to P_2 once P_2 subsidises P_3 through $l_{3\leftarrow 2}$. However, in a case of two sources, e.g. $S_0 \rightarrow P_1 \rightarrow P_2 \leftrightarrow P_3 \leftarrow S_1$, then *CM* for each population was calculated from the source giving the largest coefficient: if for P_2, $CM\text{-}_{S1} = l_{3\leftarrow S1} \cdot l_{2\leftarrow 3} > l_{1\leftarrow S0} \cdot l_{2\leftarrow 1} = CM\text{-}_{S0}$ then we chose $CM\text{-}_{S1}$ for population P_2 because $CM\text{-}_{S1} > CM\text{-}_{S0}$. Appendix S2 (Section 2.3) gives detailed information about connectivity coefficients used to calculate *CM*.

Importantly, *CM* is influenced by the position of the focal population downstream of the sources and on whether the network is either "stepping stone" (Carr and Reed 1993) or "small world" type (Watts and Strogatz 1998; i.e. networks where populations are highly connected with each other). Here we also used the coefficient of determination (R^2) as a metric of effect sizes based on both the raw data and log-transformed recovery times, i.e. $\log(T_{50})$ and log-transformed values of *CM*.

Results

Life history and habitat matrix

The density-dependent coefficient β did not have any important influence on recovery times (Fig 3) and it is not considered further. The term ω (the product of fecundity and survival: Fig. 2) had a strong effect on the predicted recovery times (Fig 3). At high ω ($=10^4$), the predicted recovery times were much shorter and had a lower degree of variation among larval strategies and time of larval release (April vs. August) and regions (Fig. 4). The term ω also seems to influence variability in recovery time within a region. For instance, for Cardigan Bay (Fig. 5), the simulation resulted in short recovery times (T_{50} <25 years) for all strategies with ω of 10^4, but at ω of 10 such times varied considerably among larval behaviours or sites (T_{50} varied from < 25 to

346 >100 years). Overall, the model predicted that increased fecundity and larval survival mitigates
347 the effects of larval strategies and time of release on recovery times. This conclusion is logical
348 because in equation (4), the term ω operates on settlement through a multiplicative effect (the
349 effect of the transport coefficients, $l_{j \to p}$, on settlement is increased ω -fold).

350 In the model, larval behaviour drives recovery times through changes in the coefficients of the
351 transport matrix (Fig. 2). Larval behaviour had an important effect on recovery time but this
352 effect depended on other predictors (Figs. 3, 4). In most simulations, tidal migration led to short
353 recovery times (T_{50} <25 years); under a tidal migration strategy the effects of ω (month of
354 release) were smaller than under other migration strategies, at both the scale of regions (Fig. 4)
355 and within regions (Figs. 5, 6). Passive and diel migration let to regional scale variation in
356 recovery times (Fig 6, see also Appendix S4: Figs S4-S7) from short (Irish coast: T_{50} < 5 years)
357 to longer times (e.g. Liverpool Bay: average T_{50} 20-40 and Cardigan Bay: ~ 40-70 years both ω
358 = 10). Taken together, tidal migration and high fecundity/larval survival (i.e. high ω) minimised
359 the average and the spatial and temporal variability in recovery time.

360 There was also important regional scale and temporal variation in recovery times (Fig 3 and 4),
361 driven by oceanography. The Irish coast showed consistently short recovery times (Fig. 6); i.e.
362 they were short irrespective of tidal strategy and month of larval release. By contrast, recovery
363 in other regions was largely affected by tidal strategy and month of release. In addition, recovery
364 times were slightly shorter in simulations of release in April as compared with those in August
365 (Figs. 4, 5).

366

367

Network topology

Network topology refers to the geometric arrangement of the network (Kininmonth et al. 2010) including its nodes and connections. A key question was whether local subsidies and retention coefficients, constituting direct connections to each population, were able to explain the patterns of recovery time. Subsidy and retention were poor as predictors of recovery time ($R^2<0.10$), although the transport coefficients defining such connections determined recovery times by design (Fig. 2). In general, populations characterised by high subsidy recovered rapidly but recovery time varied considerably when subsidy was low (Fig. 7a); examination of scatterplots showed that subsidy (or retention) had a weak relationship with recovery time (exception: combination tidal strategy, August release, $\omega = 10$: Appendix S4, Figs. S12 and S13). By contrast, total connectivity (*CT*) or the maximum connectivity to the source populations outside the area of extinction (*CM*) were a strong predictor of recovery times ($R^2 > 0.7$; Fig. 7b,c).

CM represent the connectivity provided by one of the paths considered in *CT*. Close examination of populations within regions shows how *CM* reflects the overall topology of the regional networks as modified by larval behaviour and month of larval release. For instance, the sub-network of Cardigan Bay (Populations 4-8; Fig. 5) was characterised by a stepping stone pattern where populations 6 to 8 (P_{6-8}) usually received larvae from P_{1-3}, outside the network, through P_{4-5}. For the spring simulation, in spite of differences associated with larval behaviour, all connectivity coefficients were moderate to high (mostly $> 10^{-7}$), and populations recovered quickly from extinction. However, for the summer simulation, low connectivity coefficients (mostly $<10^{-7}$) characterised the passive and diel strategies. In summer, the differences in

recovery times among populations were high as extremely low recovery rates were predicted for some locations but not others. For example, for passive dispersal, P_7 has a long predicted recovery rate (T_{50} >100 years) compared with the adjacent site P_5 (rapid recovery: T_{50} < 5 years) despite similar levels of subsidy (10^{-7} vs ~10^{-8}). However, P_5 is strongly and directly connected with a population (P_3), located outside the area of extinction (connectivity P_3-P_5 ~ 10^{-7}) as compared with P_6 (connectivity P_3-P_6 <10^{-18}). Stepping stone patterns are not reflected in the subsidy but *CM* incorporates both the subsidy from populations that are connected to the source and the position in the network. Low values of *CM* are found in populations that are not directly connected to the sources outside the region of extinction and instead are organised stepping stone patterns. Stepping stone patterns were not present in all regions; for instance, the subnetwork of Anglesey (Fig. S5) resembles a "small world" type, especially for the passive strategy (i.e. with populations closely connected with each other and with the source). Whether the network structure resembled a stepping-stone or a small world type also depended on the larval strategy (Figs. S6, S7: Liverpool Bay and West Ireland): in particular, the tidal strategy which led to short recovery times gave rise to several connections between the source and the populations located inside the region of extinction.

Discussion

We have carried out a modelling exercise in order to better understand the role of life history strategies, the habitat matrix and the network topologies in determining the capacity of local populations to recover from extinction. Recovery in some cases took many decades; this is consistent with empirical observations of meta-populations over large regions (> 20 years: Lessios 2016); however, in our case they may reflect the fact that we simulated recovery based only on a single larval release event each year. Recovery strongly depended on the interactive

effect of trait combinations and the temporal and spatial variations in the habitat matrix. Real spatial or temporal patterns will look blurred compared with model outputs because many species will produce several batches of larvae each year and hence profit from temporal changes in hydrodynamic conditions. In addition, effects of larval strategy might be blurred because swimming speeds may not be constant over time or may vary intra-specifically according to the physiological state of larvae (e.g. body size, nutritional condition). Recovery will also be driven by Allee effects and the extent to which regional extinction lead to regime shifts in the local habitat (see Lessios 2016 for discussion). Given these points, we use our results only as a guide for understanding processes driving recovery from the standpoint of larval survival and dispersal. In our model, the characteristics of the habitat matrix were driven by oceanographic conditions and larval survival (manipulated through the term ω). The characteristics of the habitat matrix contributed to the properties of the regional sub-network, which in turn were driving recovery time; the correlation between recovery times and the connectivity to the source populations outside the region of extinction suggested that recovery is driven by whole network properties.

Life history strategies

High fecundity and tidal transport minimised recovery times. High fecundity is known to increase connectivity (Johansson et al. 2012, Treml et al. 2012) but fecundity varies considerably among marine species (Ramirez-Llodra 2002). Under the conditions of the model, only the most fecund species (producing ~10^6 larvae per female) would be able to produce sufficient survivors to ensure quick recovery (T_{50}<5 years) irrespective of region and season. Less fecund species may however avoid low recovery rates by producing multiple broods and releasing larvae over a protracted period.

435 Our model predicts that not only high fecundity but also tidal migration can lead to short
436 recovery times. In the sea, larval vertical migration vary across species (Shanks and Brink 2005;
437 Epifanio and Cohen 2016) even within the same habitat (Lindley et al. 1994; Garrison 1999).
438 While tidal migrations usually promote transport, diel migration can promote retention (e.g.
439 Shanks 2009; Queiroga et. al 2007); hence, one would expect that variations in larval strategies
440 among species would lead to important intraspecific variation in recovery times. Our models
441 however do not include the fact that diel migrations reduce mortality by predation (Hays 2003)
442 and would indirectly contribute to shorter recovery times.

443 The finding that dispersal strategies can be as important as high fecundity is relevant from the
444 evolutionary standpoint. First, K-strategists, characterised by low fecundity, but possessing the
445 appropriate pattern of larval migration, would be able to quickly recolonise habitats post-
446 disturbance. Second, larval behaviour may provide an evolutionary routes to maximise
447 connectivity (and hence fitness), free from constraints associated with increased fecundity.
448 Because of energetic constraints, fecundity is linked through a trade-off with per-offspring
449 investment (Marshall et al. 2007; Kindsvater and Otto 2014). Because maximising fecundity will
450 come at the costs of reducing larval survival, species may not be able to increase fitness through
451 increments in ω *(= fecundity* × *larval survival).* However, if specific behavioural strategies are
452 not linked to the energetic constraints, then fitness can be increased through increments in the
453 larval transport coefficients. The phenotypic links characterising the life histories of marine
454 organisms (Marshall and Morgan 2011) predict that selective pressures in the adult habitat may
455 well drive the evolution of larval behaviour, or alternatively that selection for specific larval
456 behaviours (e.g. for diel migration) may drive the evolution of fecundity and offspring size.

457 Advance in this field needs information about the covariation between per offspring investment,
458 larval swimming speed and behavioural strategies.

459 The effect of life history variation on recovery times modelled here are also relevant to
460 understand the structure of meta-communities. When local communities are structured through
461 priority effects, such trait combinations may determine which species are established first, and
462 which may inhibit or promote the establishment of a second species (Almany 2003, Chase 2007).
463 Depending on trait combinations, conditions of the habitat matrix may lead to trait-based
464 environmental filtering (Lebrija-Trejos et al. 2010). Environmental filtering would occur because
465 disturbance would select species according to traits promoting rapid recovery, e.g. high fecundity
466 (Ponge 2013, Seifan et al. 2013) or specific migration strategies. Because the importance of
467 migration strategies depends on properties of the habitat matrix (e.g. oceanographic conditions in
468 our specific case), our models indicate that structure of metacommunities may depend on
469 landscape-dispersal interactions. Landscape-dispersal interaction have been pointed as an
470 overlooked but potentially important driver of metacommunity structure (Ryberg and Fitzgerald
471 2016).

472 **Role of habitat matrix and network topology**

473 Our model outputs reinforce the finding by others concerning the role of the habitat matrix in
474 driving recovery (Hanski 1999, Joly et al. 2001, Haynes and Cronin 2004, Fisher et al. 2005,
475 Goodsell and Connell 2005). A component of the habitat matrix is given by those factors driving
476 larval survival (Shima and Swearer 2009), incorporated as η, in the term ω. Our findings are
477 consistent with arguments in Paris et al. (2007) on including overall larval survival rates to

478 understand the role of connectivity on population recovery and highlight the necessity to
479 quantify larval survival in the field (Vaughn and Allen 2010, but see White et al. 2014).

480 Species traits, the quality of the habitat matrix and the spatial configurations of the local
481 populations contributes to the characteristics of the network topology through effects on the
482 transport coefficients. We found that effects of network topology on recovery were captured in
483 the connectivity to the outside source, either as the total connectivity of as the path providing the
484 maximum connectivity (*CM*) because high values of *CM* would occur more frequently in small
485 world networks than on those characterised by stepping-stone patterns. The fact that *CM* had a
486 much higher predictive power than subsidies and retention coefficients suggest focus should be
487 in understanding the ecological factors driving "emergent" network properties rather than (only)
488 on conditions surrounding local populations. Network topology varied at two scales, defining
489 regions linked by weak connections (see e.g. Cowen et al. 2006 as a similar example) and groups
490 of weakly connected locations within regions. Reduced larval connectivity among regions and
491 some stepping stone patterns within regions occurred at the time of formation of frontal zones
492 and thermoclines in summer, which act as conduits of larval transport (Robins et al. 2013). On
493 the other hand, strong currents promoted a small world type of network in East Ireland. Hence, it
494 seems that the nature of the habitat matrix is such that it leads to context-dependent recovery.

495 Overall, we have found high levels of contingency in attempting to determine which biological
496 and physical factors drive recovery from extinction. Key drivers of contingency were the
497 temporal variation and spatial heterogeneity of the habitat matrix given by variation hydrology;
498 the effect of habitat heterogeneity on recovery was exacerbated under low fecundity or high
499 larval mortality. Having the right larval behavioural strategy may be as important as high
500 fecundity or low mortality rates in achieving quick recovery time in a heterogeneous habitat.

Quick recovery was obtained by a strategy providing sufficient connectivity but limited overdispersion (exemplified by the tidal strategy) which led to small-world type of networks. A strategy maximising retention (here exemplified by diel vertical migration) at expenses of larval connectivity may not ensure quick recovery, unless it is coupled with high fecundity or low larval mortality. Mixed approaches, based on the application of general metapopulation models to situations characterised by realistic seascapes (exemplified by the Irish Sea) might further contribute to understand the mechanisms driving recovery from extinction after disturbance events. This is also relevant for conservation and for understanding invasion dynamics. For instance, the optimization of networks of protected areas, which depend on understanding patterns of retention and connectivity (Planes et al. 2009), would require knowledge species trait combinations. In addition, conservation should address the quality of the habitat matrix (see also Shima and Swearer 2009), which depends on stressors (e.g. pollutants, toxic algae: Vasas et al. 2007, Shaber and Sulkin 2007, predatory jellyfish: Purcel 2011, Lee et al 2013). These are the ecological and anthropogenic factors that co-determine whole network topological properties and influence recovery from extinction.

Acknowledgements

The project was partly funded by the European Union Regional Development Fund (ERDF) under the Ireland Wales Programme 2007–2013 Interreg 4A (Project 042), the Atlantic Area Programme 2017-2020 ("COCKLES": EAPA_458/2016), and the European Fisheries Fund. Modelling resources were provided by Supercomputing-Wales (https://www.supercomputing.wales/) and the SEACAMS project (Grant number 80366, 2010-

2015), funded by the Welsh Government, the Higher Education Funding Council for Wales, the Welsh European Funding Office, and the European Regional Development Fund Convergence Programme.

REFERENCES

Almany, G.R. 2003. Priority effects in coral reef fish communities. Ecology 84:1920.

Armsworth, P.R. 2002. Recruitment limitation, population regulation and larval connectivity in reef fish metapopulations. Ecology 83:1092-1104.

Artzy-Randrup, Y. and L. Stone. 2010. Connectivity, cycles, and persistence thresholds in metapopulation networks. PLOS Comp. Biol. 6:e1000876.

Ayata, S.-D., P. Lazure, and É. Thiébaut. 2010. How does the connectivity between populations mediate range limits of marine invertebrates? A case study of larval dispersal between the Bay of Biscay and the English Channel (North-East Atlantic). Progr. Oceanogr.87:18-36.

Bishop, M. J., J. A. Rivera, E. A. Irlandi, J. W. G. Ambrose, and C. H. Peterson. 2005. Spatio-temporal patterns in the mortality of bay scallop recruits in North Carolina: investigation of a life history anomaly. J. Exp. Mar. Biol. Ecol. 315:127-146.

Botsford, L. W., J. W. White, M.-A. Coffroth, C. B. Paris, S. Planes, T. L. Shearer, S. R. Thorrold, and G. P. Jones. 2009. Connectivity and resilience of coral reef metapopulations in marine protected areas: matching empirical efforts to predictive needs. Coral Reefs 28:327-337.

Burrows, M. T., D. S. Schoeman, A. J. Richardson, J. G. Molinos, A. Hoffmann, L. B. Buckley, P. J. Moore, C. J. Brown, J. F. Bruno, C. M. Duarte, B. S. Halpern, O. Hoegh-Guldberg, C. V.

544 Kappel, W. Kiessling, M. I. O'Connor, J. M. Pandolfi, C. Parmesan, W. J. Sydeman, S. Ferrier,
545 K. J. Williams, and E. S. Poloczanska. 2014. Geographical limits to species-range shifts are
546 suggested by climate velocity. Nature 507:492-495.

547 Carr, M.H. and D.C. Reed, 1993. Conceptual issues relevant to marine harvest refuges -
548 Examples from temperate reef fishes. Canadian Journal of Fisheries and Aquatic Sciences
549 50:2019-2028.

550 Chase, J.M., 2007. Drought mediates the importance of stochastic community assembly. Proc.
551 Natl. Acad. Sci. 104:17430-17434.

552 Cohen, J.C. and R. Forward Jr. 2009. Zooplankton diel vertical migration: a review of proximate
553 control. Oceanogr. Mar. Biol. Annu. Rev. 47:77-109.

554 Coma, R., M. Ribes, E. Serrano, E. Jiménez, J. Salat, and J. Pascual. 2009. Global warming-
555 enhanced stratification and mass mortality events in the Mediterranean. Proc. Natl. Acad. Sci.
556 106:6176-6181.

557 Connolly, S.R. and Roughgarden, J. 1998. A latitudinal gradient in northeast Pacific intertidal
558 community structure: evidence for an oceanographically based synthesis of marine community
559 theory Am. Nat. 151:311-326.

560 Cowen, R.K., C.B. Paris, and Srinivasan, A. 2006. Scaling of connectivity in marine populations.
561 Science 311:522-527.

562 Cowen, R. K., and S. Sponaugle. 2009. Larval dispersal and marine population connectivity.
563 Ann. Rev. Mar. Sci. 1:443-466.

564 Di Lorenzo, E. and Mantua, N. 2016. Multi-year persistence of the 2014/15 North Pacific marine
565 heatwave. Nat. Clim. Change 6:1042-1047.

566 Diaz, R. and R. Rosenberg. 2008. Spreading dead zones and consequences for marine
567 ecosystems. Science 321:926-929.

568 Elith, J., J.R. Leathwick and T. Hastie. 2008. A working guide to boosted regression trees. J.
569 Anim. Ecol. 77: 802-813.

570 Epifanio, C. E., and J. H. Cohen. 2016. Behavioral adaptations in larvae of brachyuran crabs: A
571 review. J. Exp. Mar. Biol. Ecol. 482:85-105.

572 Galecki, A. and T. Burzykowski T. 2013. Linear mixed-effect models using R. Heidelberg:
573 Springer.

574 Garrison, L. P. 1999. Vertical migration behavior and larval transport in crabs. Mar. Ecol. Prog.
575 Ser. 176:103-113.

576 Glynn, P. W. 1993. Coral reef bleaching: ecological perspectives. Coral Reefs 12:1-17.

577 Goodsell P, and S.D Connell. 2005. Historical configuration of habitat influences the effects of
578 disturbance on mobile invertebrates. Mar. Ecol. Prog. Ser. 299:79-87.

579 Hastings, A. and L.W. Botsford. 2006. Persistence of spatial populations depends on returning
580 home. Proc. Natl. Acad. Sci.103:6067.

581 Hays, G.C. 2003. A review of the adaptive significance and ecosystem consequences of
582 zooplankton diel vertical migrations. Hydrobiologia 503:163-170.

583 Hanski, I. and O.E. Gaggiotti eds. 2004. Ecology, genetics, and evolution of metapopulations.
584 Amsterdam: Elsevier Academic Press.

585 James, G., D. Witten, T. Hastie and R. Tibshirani.2013. An introduction to statistical learning
586 with applications in R. Springer.

587 Joly, P.C., A. Lehmann and O. Grolet. 2001. Habitat matrix effects on pond occupancy in newts
588 Cons. Biol.15:239-248.

589 Johansson, V., T. Ranius, and T. Snäll. 2012. Epiphyte metapopulation dynamics are explained
590 by species traits, connectivity, and patch dynamics. Ecology 93:235-241.

591 Kininmonth. S., M. Drechsler, , K. Johst, and H.P. Possingham. 2010. Metapopulation mean life
592 time within complex networks. Mar. Ecol. Prog. Ser. 417:139-149.

593 Kindsvater, H. K., D. C. Braun, S. P. Otto, and J. D. Reynolds. 2016. Costs of reproduction can
594 explain the correlated evolution of semelparity and egg size: theory and a test with salmon. Ecol.
595 Lett. 19:687-696.

596 Le Corre, N., L. E. Johnson, G. K. Smith, and F. Guichard. 2015. Patterns and scales of
597 connectivity: temporal stability and variation within a marine metapopulation. Ecology 96:2245-
598 2256.

599 Lebrija-Trejos, E., E.A.Pérez-García, J.A. Meave, F. Bongers, and L. Poorter. 2011 Functional
600 traits and environmental filtering drive community assembly in a species-rich tropical system.
601 Ecology 91:386-398.

602 Lee, P.L.M., M.N.Dawson, S.P. Neill, P.E. Robins, J.D.R. Houghton, T.K. Doyle, G.C. Hays.
603 2013. Identification of genetically and oceanographically distinct blooms of jellyfish. J. R. Soc.
604 Int. 10:20120920.

605 Lessios, H. A. 2016. The Great *Diadema antillarum* die-off: 30 years later. Annu. Rev. Mar. Sci.
606 8:267-283.

607 Lett, C., T. Nguyen-Huu, M. Cuif, P. Saenz-Agudelo, and D. M. Kaplan. 2015. Linking local
608 retention, self-recruitment, and persistence in marine metapopulations. Ecology 96:2236-2244.

609 Levin, L. A. 2006. Recent progress in understanding larval dispersal: new directions and
610 digressions. Integr. Comp. Biol. 46:282-297.

611 Lindley, J. A., R. Williams, and D. V. P. Conway. 1994. Variability in dry weight and vertical
612 distributions of decapod larvae in the Irish Sea and North Sea during the spring. Mar. Biol.
613 120:385-395.

614 Malham, S.K., T.H. Hutchinson and M. Longshaw. 2012. A review of the biology of European
615 cockles (*Cerastoderma* spp.). J. Mar. Biol. Ass. U. K. 92:1563-1577.

616 Marshall, D.J., M.J. Keough, and W.S. David. 2007. The evolutionary ecology of offspring size
617 in marine invertebrates. Adv. Mar. Biol. 53:1-60.

618 Marshall D.J. and S.G. Morgan. 2011. Ecological and evolutionary consequences of linked life-
619 history stages in the sea. Current Biol. 21: R718–R725

620 Miller, R. J. and A. G. Colodey, 1983. Widespread mass mortalities of the green sea urchin in
621 Nova Scotia. Mar. Biol. 73:263-267.

622 Morel-Journel, T., P. Girod, L. Mailleret, A. Auguste, A. Blin, and E. Vercken. 2016. The highs
623 and lows of dispersal: how connectivity and initial population size jointly shape establishment
624 dynamics in discrete landscapes. Oikos 125:769-777.

625 North, E. W., Z. Schlag, R. R. Hood, M. Li, L. Zhong, T. Gross, and V. S. Kennedy. 2008.
626 Vertical swimming behavior influences the dispersal of simulated oyster larvae in a coupled
627 particle-tracking and hydrodynamic model of Chesapeake Bay. Mar. Ecol. Prog. Ser. 359:99-
628 115.

629 Paris, C.B., L.M. Chérubin and R.K. Cowen. 2007. Surfing, spinning, or diving from reef to reef:
630 effects on population connectivity. Mar. Ecol. Prog. Ser. 347:285-300.

631 Pinheiro, J. and D. Bates. 2000. Mixed effects models in S and S plus. Springer New.

632 Pinheiro J, D. Bates, S. DebRoy, D. Sarkar and R Core Team. 2018. nlme: Linear and nonlinear
633 mixed effects Models. R package version 3.1–131.1, https://CRAN.R–project.org/package=nlme.

634 Planes, S., G.P. Jones and S.R. Thorrold. 2009. Larval dispersal connects fish populations in a
635 network of marine protected areas. Proc. Natl. Acad. Sci.106:5693-5697.

636 Ponge, J.-F. 2013. Disturbances, organisms and ecosystems: a global change perspective. Ecol.
637 Evol. 3:1113-1124.

638 Purcell, J.E. 2011. Jellyfish and ctenophore blooms coincide with human proliferations and
639 environmental perturbations. Annu. Revi. Mar. Sci. 4:209-235.

640 Queiroga, H., T. Cruz, A. dos Santos, J. Dubert, J. I. Gonzalez-Gordillo, J. Paula, A. Peliz, and
641 A. M. P. Santos. 2007. Oceanographic and behavioural processes affecting invertebrate larval
642 dispersal and supply in the western Iberia upwelling ecosystem. Progr. Oceanogr. 74:174-191.

643 Ramirez Llodra E. 2002. Fecundity and life-history strategies in marine invertebrates. Adv. Mar.
644 Biol. 43:87-170.

645 Robins P. E., S.P.Neill., L. Giménez, S. R. Jenkins and S. K. Malham. 2013. Physical and
646 biological controls on larval dispersal and connectivity in a highly energetic shelf sea. Limnol.
647 Oceanogr. 58:505-524.

648 Robins, P. E., M. W. Skov, M. J. Lewis, L. Giménez, A. G. Davies, S. K. Malham, S. P. Neill, J.
649 E. McDonald, T. A. Whitton, S. E. Jackson, and C. F. Jago. 2016. Impact of climate change on
650 UK estuaries: A review of past trends and potential projections. Estuar. Coast. Shelf Sci.
651 169:119-135.

652 Ryberg, W. A., and L. A. Fitzgerald. 2016. Landscape composition, not connectivity, determines
653 metacommunity structure across multiple scales. Ecography 39:932-941.

654 Rumrill, S.S. 1990. Natural mortality of marine invertebrate larvae. Ophelia 32:163-198.

655 Seifan, M., Seifan, T., Schiffers, K., Jeltsch, F. and Tielbeger, K. 2013. Beyond the Competition-
656 colonization trade-off: linking multiple trait response to disturbance characteristics. Am. Nat.
657 181:151-160.

658 Shaber, K. and S. Sulkin. 2007. Feeding on dinoflagellates by intermediate and late stage crab
659 zoeae raised in the laboratory and collected from the field. J. Exp. Mar. Biol. Ecol. 340, 149-
660 159.

661 Shanks, A. L. 2009. Pelagic larval duration and dispersal distance revisited. Biol. Bull. 216:373-
662 385.

663 Shanks, A. and L. Brink. 2005. Upwelling, downwelling, and cross-shelf transport of bivalve
664 larvae: test of a hypothesis. Mar. Ecol. Prog. Ser. 302:1-12.

665 Shima, J.S. and S.E. Swearer. 2009. Larval quality is shaped by matrix effects: implications for
666 connectivity in a marine metapopulation. Ecology 90:1255-1267.

667 Tollefson, J. 2016. Epic El Nino yields massive data trove. Nature 531:20-21.

668 Treml, E.A., J.R. ford, K.P. Black, S.E. Swearer.2015. Identifying the key biophysical drivers,
669 connectivity outcomes, and metapopulation consequences of larval dispersal in the sea. Mov.
670 Ecol 3:17

671 Treml, E.A., J.J. Roberts, Y.Chao, P.N. Halpin, H.P. Possingham and C. Riginos, 2012.
672 Reproductive output and duration of the pelagic larval stage determine seascape-wide
673 connectivity of marine populations. Integr. Comp. Biol. 52:525-537.

674 Turner, M. G. 2010. Disturbance and landscape dynamics in a changing world. Ecology
675 91:2833-2849.

676 Vaughn, D. and J.D. Allen. 2010. The peril of the plankton. Integr. Comp. Biol. 50:552-570.

677 Vasas V, C. Lancelot, V. Rousseau and F. Jordán. 2007. Eutrophication and overfishing in
678 temperate nearshore pelagic food webs: a network perspective. Mar. Ecol. Prog. Ser. 336:1-14.

679 Watts, D.J. and S.H. Strogatz. 1998. Collective dynamics of 'small-world' networks. Nature
680 393:440–442.

681 White, J.W., S.G. Morgan and J.L. Fisher. 2014. Planktonic larval mortality rates are lower than
682 widely expected. Ecology 95:3344-3353.

683 Wiens, J. A. 1997. Metapopulation dynamics and landscape ecology. Pp 43-68 in I. Hanski and
684 M. E. Gilpin [eds]. Metapopulation biology. Academic Press, San Diego.

685 Woodley, J., E. A. Chornesky, , P. A. Clifford, J. B. C. Jackson, , L. S. Kaufman, N. Knowlton,
686 J. C. Lang, M. P. Pearson, J. W. Porter, M. C. Rooney, K. W. Rylaarsdam, V. J. Tunnicliffe, C.
687 M. Wahle, J. L. Wulff, A. S. G. Curtis, M. D. Dallmeyer, B. P. Jupp, M. A. R. Koehl, J. Neigel,
688 E. M. Sides. 1981. Hurricane Allen's impact on Jamaican coral reefs. Science 214:749-61.

689 White, J.W., A. Rassweiler, J.F. Samhouri, A.C. Stier and C. White. 2014. Ecologists should not
690 use statistical significance tests to interpret simulation model results. Oikos 123:385-388.

691 Zuur, A., Ieno, E., Walker, N., Savaliev, A. & Smith, G. 2009. Mixed effect models and
692 extensions in ecology with R. New York: Springer.

693

694

695

696 **Figure captions**

697

698 Figure 1. The model domain, the Irish Sea, with the spatial location of the local populations and
699 the four areas of extinction (A: Cardigan Bay, B: Anglesey; C: Liverpool Bay and D: Irish coast).
700 Arrows indicate the main pathways of connectivity among regions, depending on the larval
701 strategy (passive, tidal, diel) as obtained in Robins et al (2013).

702 Figure 2. Flow diagram summarising the relationships between factors or natural drivers defining
703 the habitat matrix, the traits and the terms or coefficients determining the recovery time (T_{50}). The
704 habitat matrix is characterised by biotic and abiotic factors, affecting larval survival (manipulated
705 here variations in the term ω) and by oceanographic conditions driving larval transport and hence
706 the coefficients of the connectivity matrix. The traits are the fecundity (contributing to the term
707 ω) and larval behaviour (contributing to the coefficients of the connectivity matrix). The term ω
708 is the product of larval survival and fecundity; l_{ij} denotes the coefficients of the transport matrix.

709 Figure 3. Importance of region, larval strategy (Str), ω, Month of release, and β for recovery time
710 from extinction (T_{50}). (a) Percent influence estimated from boosted regression trees. (b) Difference
711 between parameter estimates at predictor levels vs the reference, estimated from general least
712 squares model (from summary output, total of 96 parameters). In (b) the references correspond to
713 ω =10, β =0.0001, Month = April, Dispersal = passive, region = Cardigan bay. Each dot
714 corresponds to the difference between the reference level and another level, for a given
715 combination of predictors. For instance, for ω the additional level is ω =10,000 and there are 48
716 dots corresponding to the combinations of levels of all other predictors (region, β, month and
717 strategy: 48 = 4x2x2x3). For ω, β and month there is a single column of symbols because there is
718 only a single level other than the reference. Notice in (a) that β is the predictor with less relative

719 influence; in (b) this coincides with almost no difference between parameter estimates obtained at
720 the reference (β =0.1) vs. β =0.0001 irrespective of remaining predictors (most dots are on the zero
721 line). By contrast, ω has a strong relative influence (a); (b) shows that differences vary depending
722 on other predictor combinations, but they are always negative, indicating that higher ω drives
723 consistently reduced recovery time. Region (as month and strategy) had high relative importance
724 (a) but the magnitude depended on the combinations of other parameters (in b, differences are
725 negative or positive).

726 Figure 4. Average predicted recovery times (T_{50}; i.e. time required to reach 50% of asymptotic
727 population size) according to region, month of larval release, larval strategy and values of term ω
728 (representing the combined effect of survival and fecundity). Boxes and error bars represent
729 standard error and standard deviation respectively. Abbreviations: CAB: Cardigan Bay, ANG:
730 Anglesey: LIVB: Liverpool Bay, W-IRE: East Ireland.

731 Figure 5. Cardigan Bay. Left panels: Prediction of recovery times (T_{50}) under different
732 combinations of ω, larval strategies and time of larval release (β=*0.0001*). Right Panels: network
733 topologies depending on month of release and larval strategy. Boxes: populations (source
734 populations, outside the region of extinction, in light grey). Numbers associated with arrows:
735 connectivity coefficients (as order of magnitude: e.g. -3 corresponds to 10^{-3}). For simplicity, we
736 only show coefficients between adjacent populations and the highest connectivity between two
737 populations (connections are bi-directional).

738 Figure 6. Prediction of recovery times (T_{50}: time required to reach 50% of the numbers reached in
739 year 400) for all regions, under different combinations larval strategy and time of larval release
740 (ω= 10^4; β=0.0001).

741 Figure 7. Recovery time vs (a) subsidy, (b) total connectivity (CT in log-transformed scale) and
742 the maximum connectivity (CM in log-transformed scale) to sources located outside the region of
743 extinction.

744

745

746

747

748

749

750

751

752

753

754

755

756

757

758

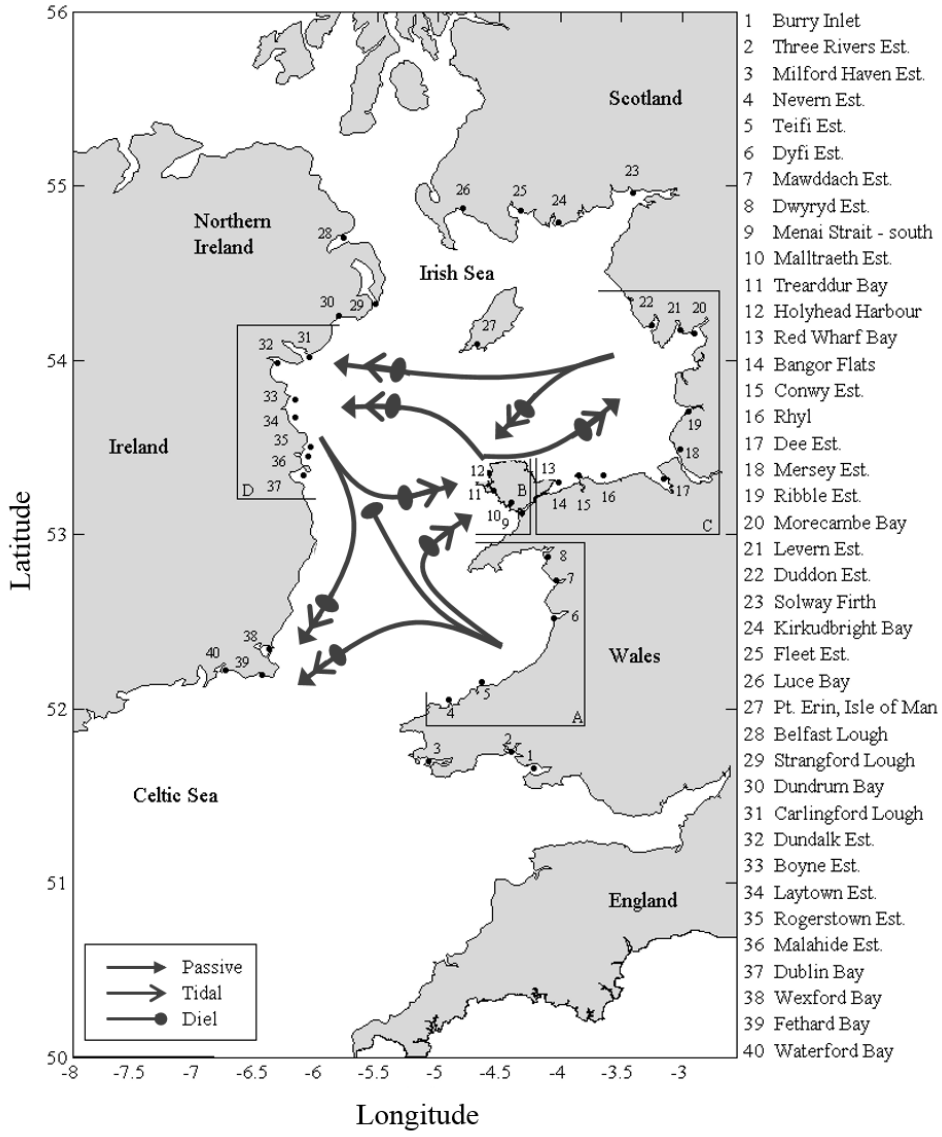

Figure 1. The model domain, the Irish Sea, with the spatial location of the local populations and the four areas of extinction (A: Cardigan Bay, B: Anglesey; C: Liverpool Bay and D: Irish coast). Arrows indicate the main pathways of connectivity among regions, depending on the larval strategy (passive, tidal, diel) as obtained in Robins et al (2013).

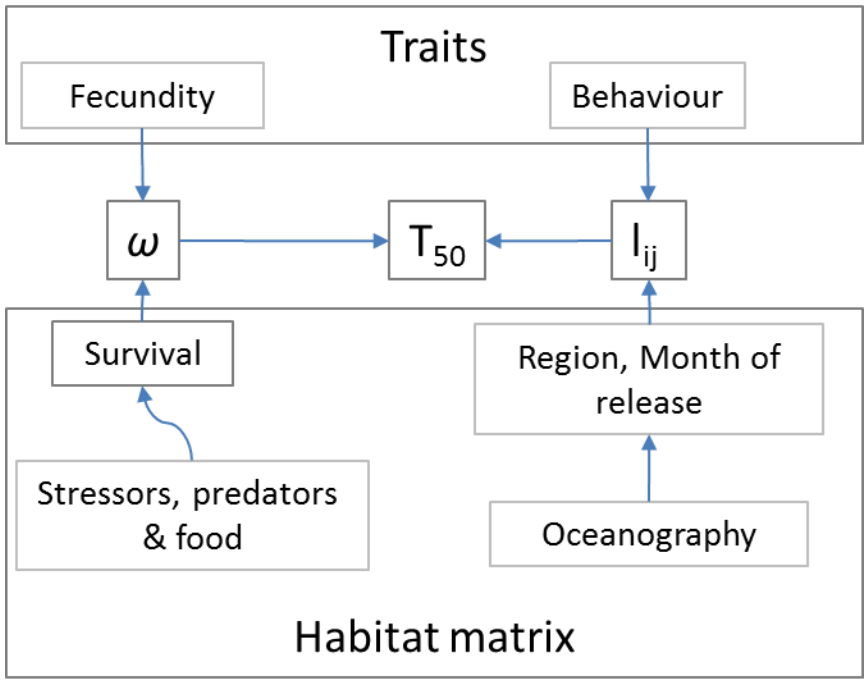

Figure 2. Flow diagram summarising the relationships between factors or natural drivers defining the habitat matrix, the traits and the terms or coefficients determining the recovery time (T_{50}). The habitat matrix is characterised by biotic and abiotic factors, affecting larval survival (manipulated here variations in the term ω) and by oceanographic conditions driving larval transport and hence the coefficients of the connectivity matrix. The traits are the fecundity (contributing to the term ω) and larval behaviour (contributing to the coefficients of the connectivity matrix). The term ω is the product of larval survival and fecundity; l_{ij} denotes the coefficients of the transport matrix.

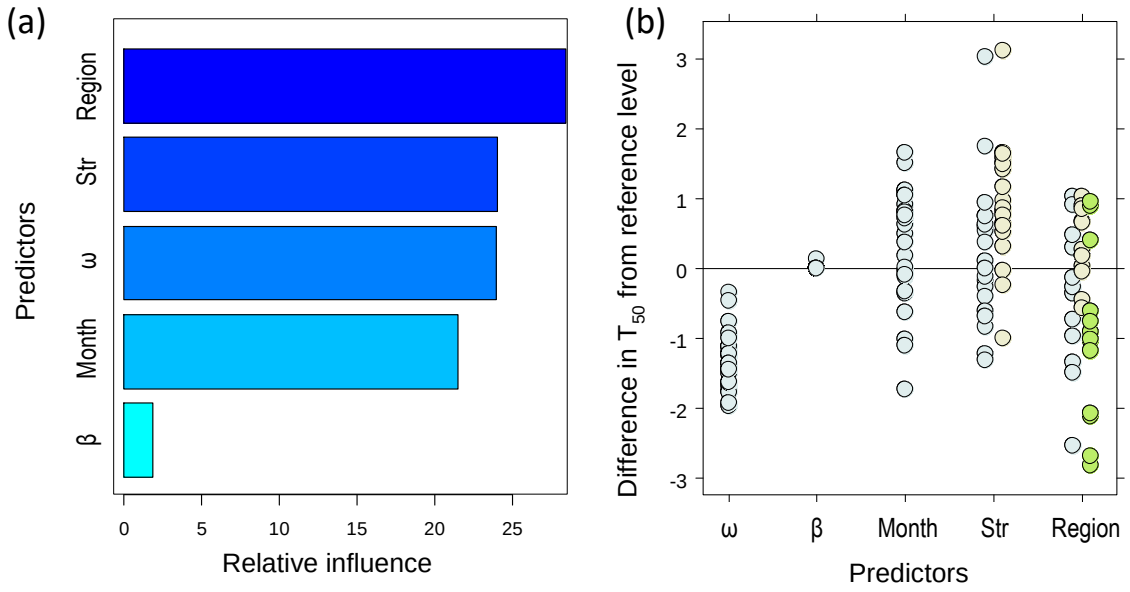

778

779 Figure 3. Importance of region, larval strategy (Str), ω, Month of release, and β for recovery time
780 from extinction (T_{50}). (a) Percent influence estimated from boosted regression trees. (b) Difference
781 between parameter estimates at predictor levels vs the reference, estimated from general least
782 squares model (from summary output, total of 96 parameters). In (b) the references correspond to
783 ω =10, β =0.0001, Month = April, Dispersal = passive, region = Cardigan bay. Each dot
784 corresponds to the difference between the reference level and another level, for a given
785 combination of predictors. For instance, for ω the additional level is ω =10,000 and there are 48
786 dots corresponding to the combinations of levels of all other predictors (region, β, month and
787 strategy: 48 = 4x2x2x3). For ω, β and month there is a single column of symbols because there is
788 only a single level other than the reference. Notice in (a) that β is the predictor with less relative
789 influence; in (b) this coincides with almost no difference between parameter estimates obtained at
790 the reference (β =0.1) vs. β =0.0001 irrespective of remaining predictors (most dots are on the zero
791 line). By contrast, ω has a strong relative influence (a); (b) shows that differences vary depending

on other predictor combinations, but they are always negative, indicating that higher ω drives consistently reduced recovery time. Region (as month and strategy) had high relative importance (a) but the magnitude depended on the combinations of other parameters (in b, differences are negative or positive).

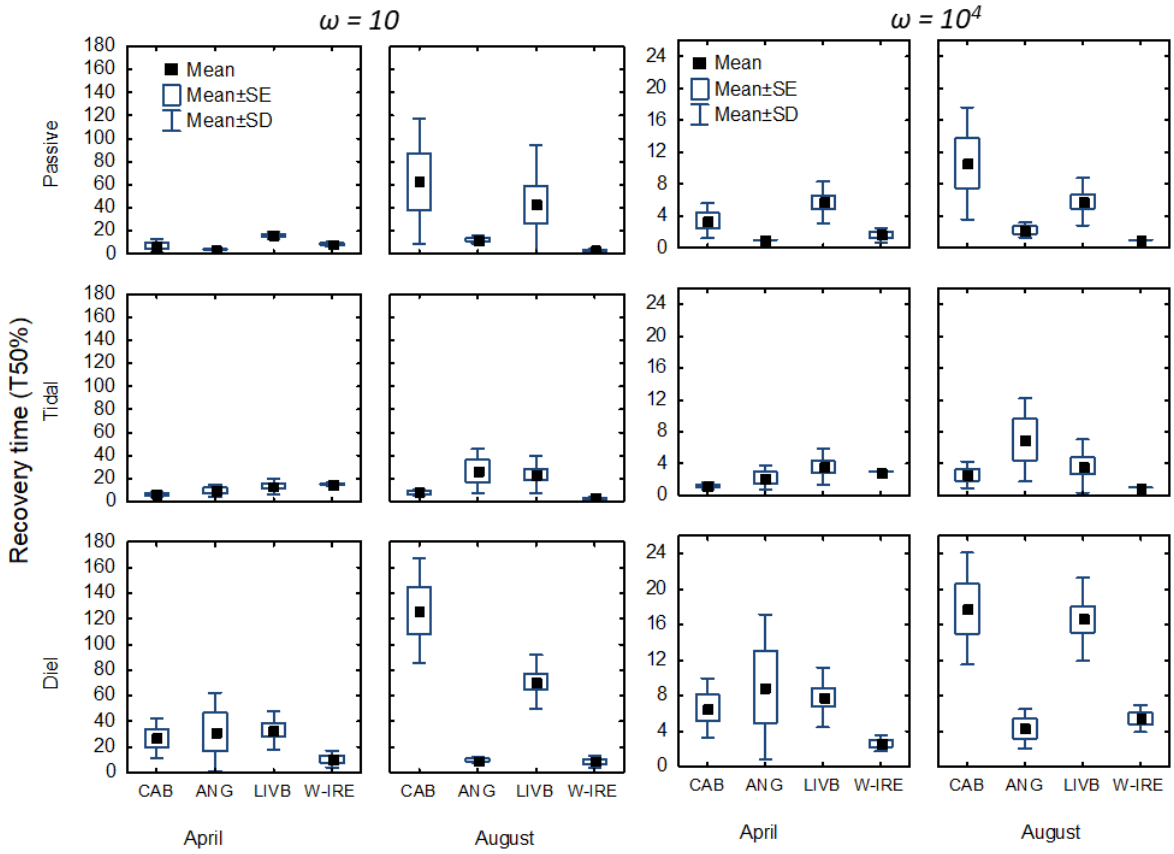

Figure 4. Average predicted recovery times (T_{50}; i.e. time required to reach 50% of asymptotic population size) according to region, month of larval release, larval strategy and values of term ω (representing the combined effect of survival and fecundity). Boxes and error bars represent standard error and standard deviation respectively. Abbreviations: CAB: Cardigan Bay, ANG: Anglesey: LIVB: Liverpool Bay, W-IRE: East Ireland.

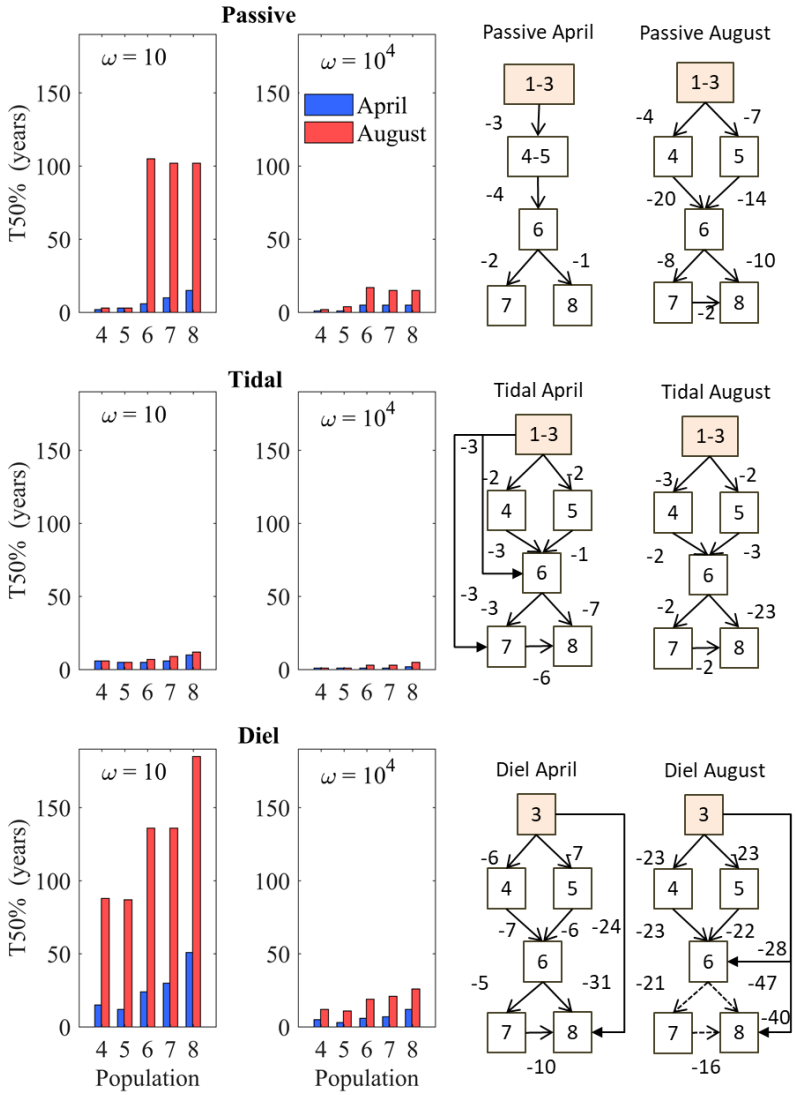

Figure 5. Cardigan Bay. Left panels: Prediction of recovery times (T_{50}) under different combinations of ω, larval strategies and time of larval release (β=*0.0001*). Right Panels: network topologies depending on month of release and larval strategy. Boxes: populations (source populations, outside the region of extinction, in light grey). Numbers associated with arrows: connectivity coefficients (as order of magnitude: e.g. -3 corresponds to 10^{-3}). For simplicity, we only show coefficients between adjacent populations and the highest connectivity between two populations (connections are bi-directional).

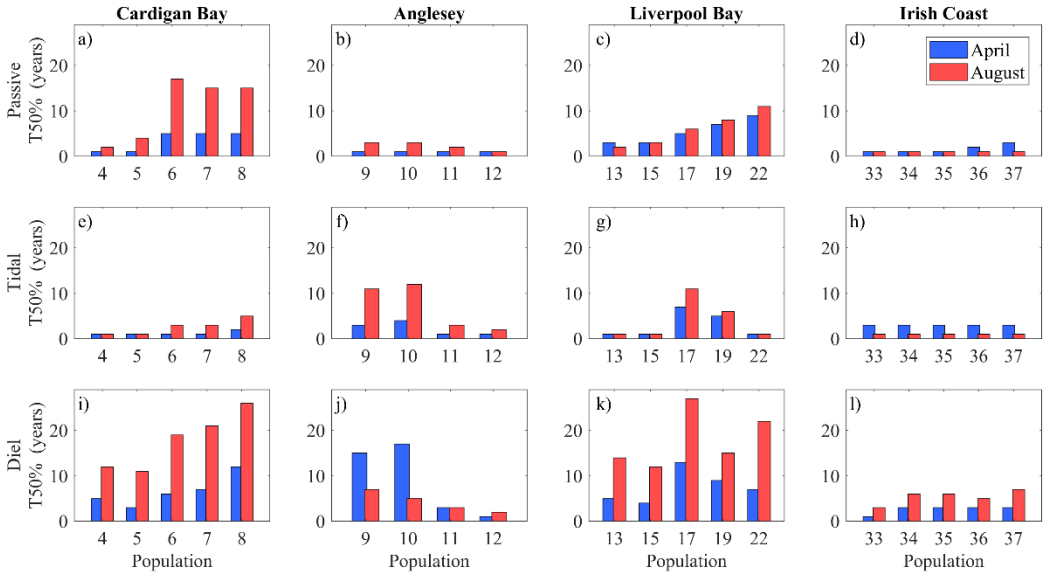

Figure 6. Prediction of recovery times (T_{50}: time required to reach 50% of the numbers reached in year 300) for all regions, under different combinations larval strategy and time of larval release ($\omega = 10^4$; $\beta = 0.0001$).

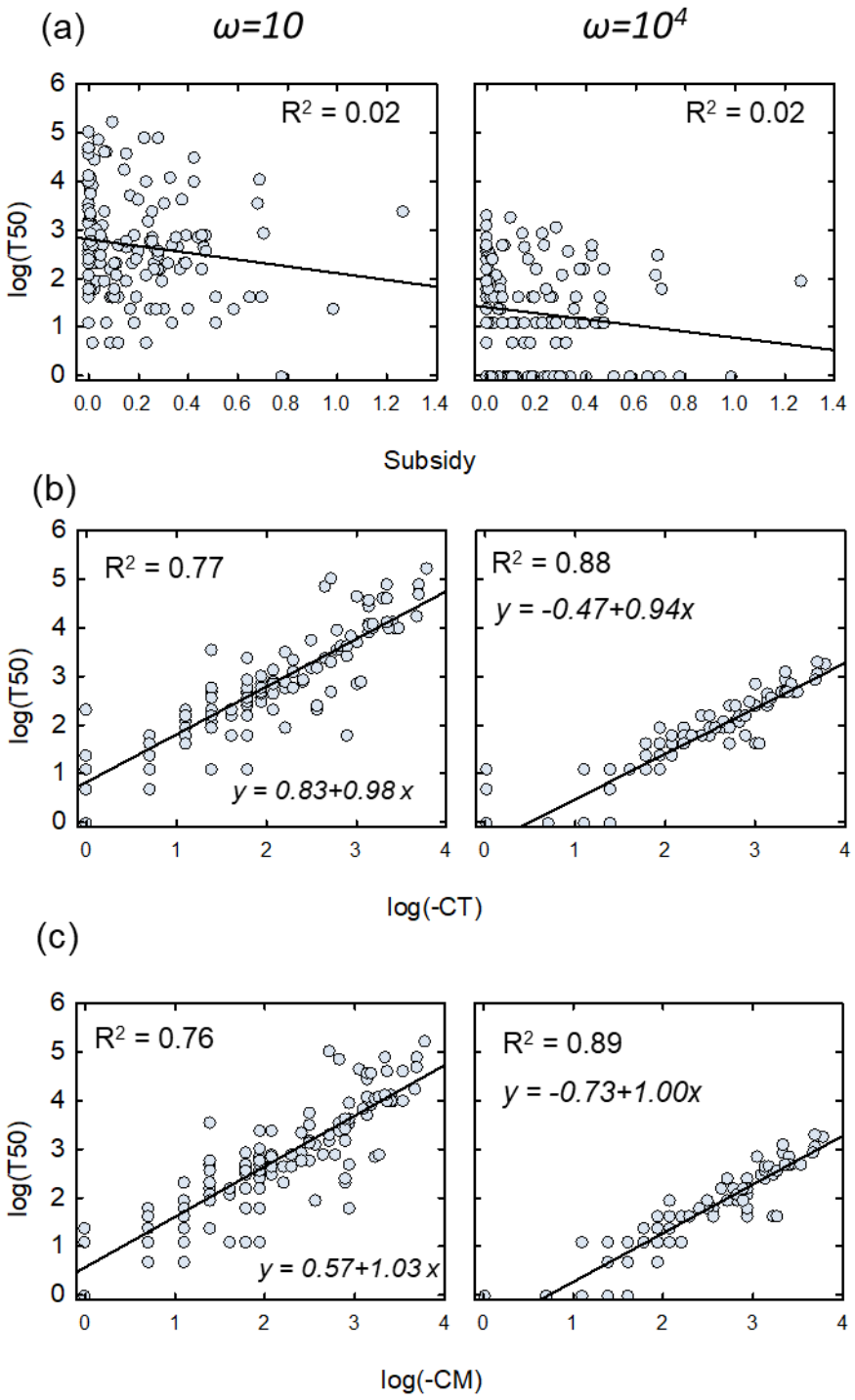

849

850 Figure 7. Recovery time vs (a) subsidy, (b) total connectivity (*CT* in log-transformed scale) and
851 the maximum connectivity (*CM* in log-transformed scale) to sources located outside the region of
852 extinction.

Role of trait combinations, habitat matrix and network topology in metapopulation recovery from regional extinction

Luis Giménez Peter Robins and Stuart Jenkins

Supplementary information

S1: Matlab code for model simulation

```
%% Role of trait combinations, habitat matrix and network topology in
%% metapopulation recovery from regional extinction
%% Luis Giménez1,2, Peter Robins1, and Stuart Jenkins1

%% 1. School of Ocean Sciences, Bangor University, LL59 5AB, Menai Bridge,
%%Isle of Anglesey, United Kingdom.
%% Biologische Anstalt Helgoland, Alfred Wegener Institute, Helmholtz Centre
%% for Polar and Marine Research, 27498 Helgoland, Germany.

%% METAPOPULATION DYNAMIC MODEL
% code by Peter Robins.
 %% SECTION 1: INITIAL MATLAB ACTIONS

clear;                      % clears current MATLAB workspace
clc;                        % clears MATLAB command history since last log-on
fclose('all');              % closes all open MATLAB files

%% SECTION 2: MODEL INPUT (section to be modified...)

% Files and directories:
id = 'M:\Myfolder\';
```

```
879 file_population_abundance   = 'Population_abundance.xls';
880 file_W              = 'W.xls';
881 file_density_numerator      = 'Density_numerator.xls';
882 file_density_denominator    = 'Density_denominator.xls';
883
884 % matrix dimensions:
885 np = 40;                    % np = number of populations
886 ny = 200;                   % ny = number of years
887 st = 5;                     % st = number of stages (years) for organism
888 survival
889 itest=1;                    % 1=Beverton-Holt, 2=Otro
890
891 % Initial population abundances:
892 P     = zeros(ny,np,st);    % Initial population abundances
893 % P(1,:,:) = xlsread([id,file_population_abundance]);
894
895 % W is the product of fecundity and larval surviva;
896 % it varies with age (due to fecundity) and population of the adults
897 % neither W nor fecundity or larval survival are density-dependent
898 w     = zeros(np,st);       % W
899 %f(:,:) = xlsread([id,file_W]);
900 for ip=1:np
901     P(1,ip,:) = [1000 0 0 0 0];
902     w(ip,:)   = [0 10000 10000 10000 10000];
903 end
904 % sum initial populations:
905 for ip=1:np
906     sum_P(ip)  = sum(P(1,ip,:));
```

```
907  end
908
909  % Maximum density-dependent survival
910  % ms(:,:)  = xlsread([id,file_density_numerator]);
911  ms    = ones(np,st+1);      % Maximum survival parameter
912
913  % Parameter in denominator of density-dependent survival
914  % pd(:,:)  = xlsread([id,file_density_denominator]);
915  pd    = ones(np,st+1)*0.0001;     % Parameter in denominator
916
917  % Initialize other arrays:
918  wc    = zeros(np,np,st);    % [W*connectivity] settlement matrix
919  wcP   = zeros(np,np,st);    % [W*connectivity*pop_abundances]
920  fsf   = zeros(np,st+1);     % Final survival function for matrix based on No
921  M     = zeros(np,np,st,st); % Metapopulation matrix
922
923  %% SECTION 3: CONNECTIVITY:
924
925  id2 = 'M:\Myfolder\IrishSeaPopulations\';
926  imat = 1;   % [C1,..,C6 = Apr,..,Sep]
927  icon = 1;
928  if(icon==0)
929      c(1,:) = [0.15 0.1 0.1];
930      c(2,:) = [0.1 0.2 0.2];
931      c(3,:) = [0.1 0.6 0.6];
932  else
933      % input Connectivity matrix:
934      load([id2,'Cpassive_28d']);
```

```
%     load([id2,'Cdiel_28d_0030ms'])
%     load([id2,'Ctidal_28d_0030ms'])
    if(imat==1); c = C1; end
    if(imat==2); c = C2; end
    if(imat==3); c = C3; end
    if(imat==4); c = C4; end
    if(imat==5); c = C5; end
    if(imat==6); c = C6; end

    % Reposition Port Erin:
    rowtemp(:,:) = c(40,:);
    c(28:40,:)   = c(27:39,:);
    c(27,:)      = rowtemp(:,:);
    coltemp(:,:) = c(:,40);
    c(:,28:40)   = c(:,27:39);
    c(:,27)      = coltemp(:,:);

    % check connectivity of all matrices:
    sumC(imat,:) = sum(c');
    c=c';
end

%% SECTION 4: CALCULATION SETTLEMENT MATRIX:
% Subsidy = W * connectivity
% self-recruitment = W * self-recruitment

% Year 1:
it = 1;
```

```
for ip=1:np
for jp=1:np
for ist=1:st
    wc(ip,jp,ist)  = w(jp,ist).*c(ip,jp);
    wcP(ip,jp,ist) = wc(ip,jp,ist).*P(it,jp,ist);
end
end
end
% sum wcP matrix:
wcptemp = zeros(np,st);
rowsum  = zeros(np,np);
sum_wcP = zeros(1,np);
for ip=1:np
    wcptemp(:,:) = wcP(ip,:,:);
    rowsum(ip,:) = sum(wcptemp');
    sum_wcP(ip)  = sum(rowsum(ip,:));
end

% One year or older individuals survive to the next year following
% density-dependent survival, with density being the total density adults
if(itest==1)
  for ip=1:np
    fsf(ip,1) = ms(ip,1)./(1+pd(ip,1)*sum_wcP(ip));
    for ist=2:st+1
    fsf(ip,ist) = ms(ip,ist)./(1+pd(ip,ist)*sum_P(ip));
    end
  end
else
```

```
    for ip=1:np
      fsf(ip,1) = (pd(ip,1)*ms(ip,1))./(ms(ip,1)+sum_fcP(ip));
      for ist=2:st+1
      fsf(ip,ist) = (pd(ip,ist)*ms(ip,ist))./(ms(ip,ist)+sum_P(ip));
      end
    end
end

%% SECTION 5: ITERATE OVER ny YEARS

for it=2:ny

% Metapopulation matrix:
for ip=1:np
for jp=1:np
for ist=1:st
    M(ip,jp,1,ist) = fsf(ip,1)*wc(ip,jp,ist);    % stage = 1
    if(ist>1)                                    % stages 2-5
        M(ip,ip,ist,ist-1) = fsf(ip,ist);
    end
end
end
end

for ip=1:np
    A = zeros(st,1);
    B = zeros(st,1);
for ist=1:st
```

```
1019        D = 0;
1020        for jp=1:np
1021            A(:) = P(it-1,jp,1:5); B(:) = M(ip,jp,ist,1:5); D = D + sum(A.*B);
1022        end
1023        P(it,ip,ist) = D;
1024    end
1025    end
1026
1027    for ip=1:np
1028        sum_P(ip) = sum(P(it,ip,:));
1029    end
1030
1031    % meta-recruitment = fecundity * connectivity
1032    % self-recruitment = fecundity * self-recruitment
1033    for ip=1:np
1034    for jp=1:np
1035    for ist=1:st
1036        wc(ip,jp,ist) = w(jp,ist)*c(ip,jp);
1037        wcP(ip,jp,ist) = wc(ip,jp,ist)*P(it,jp,ist);
1038    end
1039    end
1040    end
1041    % sum wcP matrix:
1042    for ip=1:np
1043        wcptemp(:,:) = wcP(ip,:,:);
1044        rowsum(ip,:) = sum(wcptemp');
1045        sum_wcP(ip)  = sum(rowsum(ip,:));
1046    end
```

```
1047
1048  % One year or older individuals survive to the next year following
1049  % density-dependent survival, with density being the total density adults
1050  if(itest==1)
1051    for ip=1:np
1052      fsf(ip,1) = ms(ip,1)./(1+pd(ip,1)*sum_fcP(ip));
1053      for ist=2:st+1
1054      fsf(ip,ist) = ms(ip,ist)./(1+pd(ip,ist)*sum_P(ip));
1055      end
1056    end
1057  else
1058    for ip=1:np;
1059      fsf(ip,1) = (pd(ip,1)*ms(ip,1))./(ms(ip,1)+sum_fcP(ip));
1060      for ist=2:st+1;
1061      fsf(ip,ist) = (pd(ip,ist)*ms(ip,ist))./(ms(ip,ist)+sum_P(ip));
1062      end
1063    end
1064  end
1065
1066  end % END YEAR LOOP
1067
1068  %% SECTION 6: create additional matrices for visualization
1069
1070  % sum population matrices:
1071  for it=1:ny
1072  for ip=1:np
1073      POPULATIONS(it,ip) = sum(P(it,ip,:));
1074      TOTAL_POPULATION(it) = sum(POPULATIONS(it,:));
```

```
end
end
TOTAL_POPULATION=TOTAL_POPULATION';

Pyear200 = zeros(40,5);
Pyear200(:,:) = P(200,:,:);

plot(POPULATIONS);
```

S2: Preliminary model simulations

2.1 Asymptotic behaviour and population size

We first studied the influence of the connectivity coefficients and model parameters on the asymptotic behaviour and the population size. We then used those outputs to select specific values of model parameters. The panels of Fig. S1 are maps of the populations in a space defined by the retention coefficients (diagonals in the transport matrix) and the subsidy i.e. the sum of the larval connectivity coefficients, indicating transport of larvae form any population to the focal population (retention coefficient not included). Both retention and subsidy characterise the local populations from the perspective of the contributions to recruitment. Predictions (see also Robins et al. 2013) from diel vertical migration are that retention prevails over subsidy for most populations, while this is not the case for scenarios with passive dispersal and tidal vertical migration. Seasonal patterns consist of a reduction in subsidy from spring to summer in all scenarios of larval behaviour.

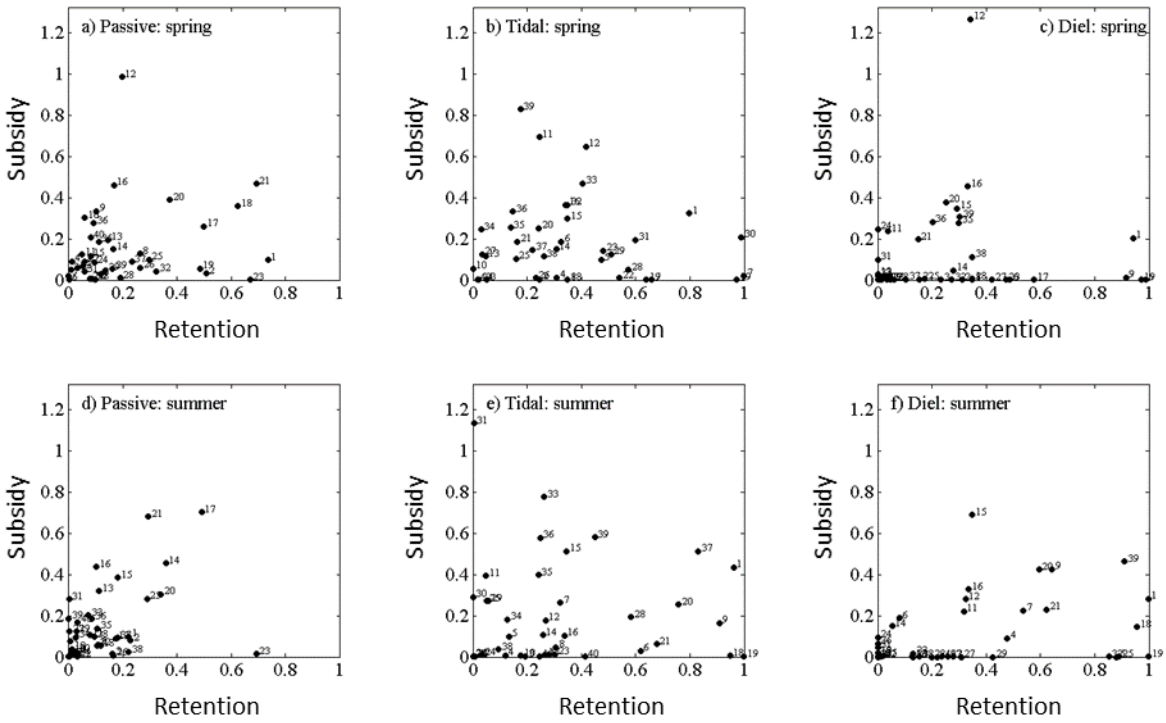

Figure S1. Map of the subsidy and retention for each population for the April and August scenarios for the passive tidal and diel strategies of larval migration. For any given population, subsidy was calculated as the sum of the connectivity coefficients indicating input of larvae from other populations (note that contrary to the retention, subsidy may by higher than 1).

Simulations showed that population size reached a near asymptotic value after ca 50 years (Fig. S2: see P_{13} as an example). No oscillations were observed, consistent with the fact that the equilibrium in this model is always stable (Armsworth 2002). These simulations give confidence that the population size observed after 200 years estimates the expected asymptotic population size.

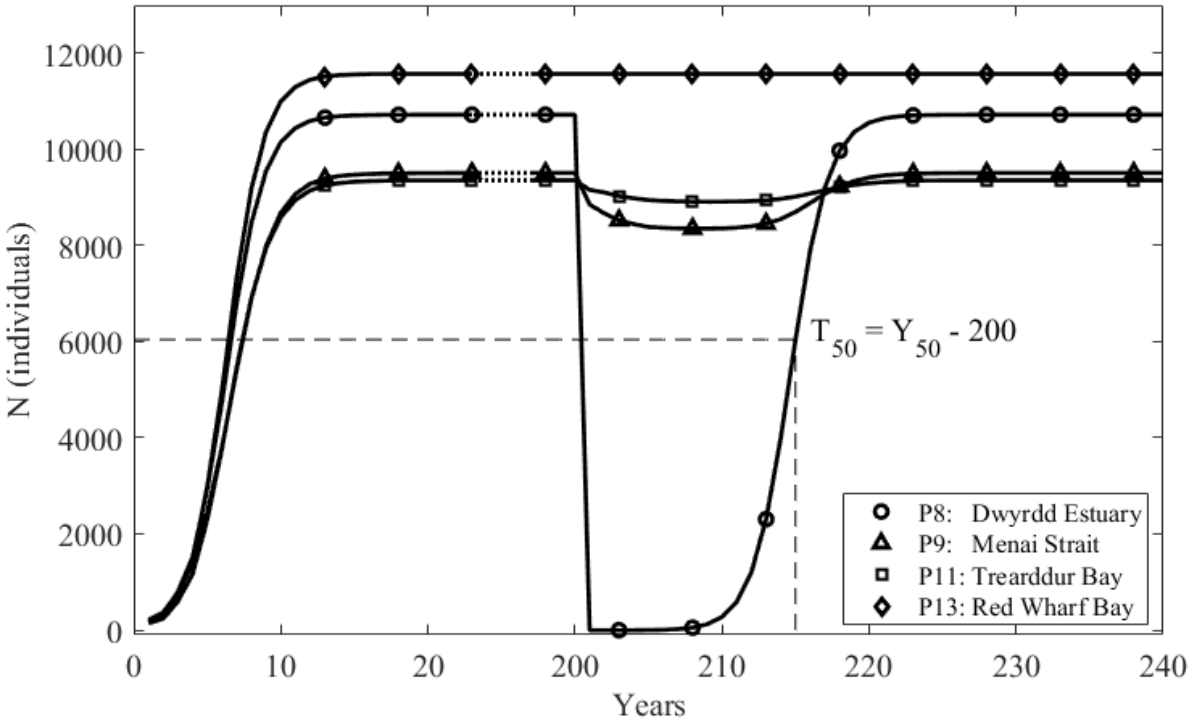

Figure S2. An example of a simulation. Models were run for 200 cycles (= years in the model) starting from 10 individuals per population. At year 201, the populations of a specific region of extinction are set to 0 (other populations are set to the numbers predicted for year 200); this is shown with P13 as example. The model is run again for further 400 years. The time of recovery is estimated as the time required to reach 50% of the numbers found after running the model for 400 years.

The asymptotic population size varied among local populations in response to ω, β and the connectivity coefficients. Taking a local population as example (Fig. S3a) models predict that the asymptotic size increase with ω (= higher fecundity or lower mortality) up to a maximum and then remain constant irrespective of ω; reductions in the strength of density-dependence (= lower β) leads to an increase in the asymptotic abundance. The asymptotic population size also depended on retention and subsidy (Fig. S3b). Low retention (compare retention in P_{22} = 0.07 vs. P_{23}= 0.67 both with subsidy < 0.01) led to low population size, as it did a low subsidy (P_{40} = 0.09 vs. P_{12} = 0.98). These results are consistent with equation 8 and elasticity analyses in Armworth (2002).

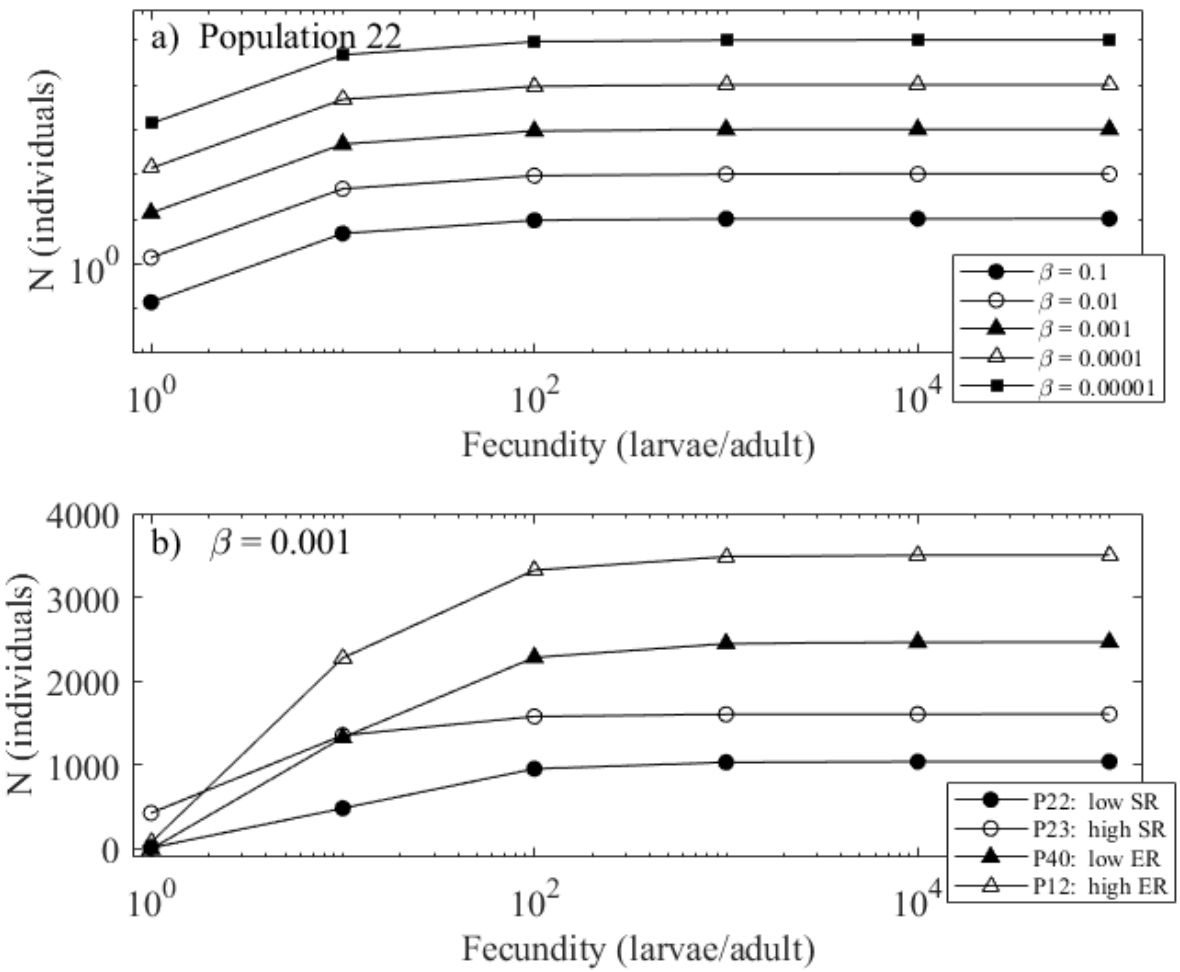

Figure S3. Examples of population sizes predicted after simulating 200 years of population dynamics. (a) Responses to fecundity and density-dependent coefficient of the Beverton-Holt model for population 22; (b) Comparisons of responses to retention and subsidy (ER) for selected populations (retention: compare P22 vs P23; subsidy: compare P12 vs P40).

2.2 Recovery when the population is rare

Here we explore drivers of recovery after extinction when the populations are at the lowest abundances. The year after extinction (on year 1), population recovery depend entirely on subsidy. All individuals on year 1 are juveniles (Table S1). On year 2, population abundance will depend on the survival of individuals present in the previous year plus new recruitment. Recruitment will still depend on subsidy because individuals start to reproduce after year 1.

Table S1 gives the equations calculating abundance discriminated by age and year after recovery. The parameters are as follows: α_1, and α_2 = density-independent survival probabilities, β = density dependent coefficient. S = is the settlement rate (eq 4 in the manuscript), which in the case of extinction it is reduced to the subsidy:

$$S = S_{t,j=p} = \omega \cdot \sum_{k=1}^{5} \sum_{j \neq p} n_{t,k,j} \cdot l_{j \to p} \text{ , (S1)}$$

Where ω is the product of fecundity and larval survival, $n_{t,k,j}$ is the abundance of organisms in the population j and age class k, and $l_{j \to p}$ are the transport coefficients between any of the j-populations and the target population p.

Table S1. Equations used to calculate rate of increase after extinction when the population is rare (i.e. one year after extinction). The rate of increase is the ratio between the total population size at t=2 versus that when t=1, i.e. N_{t2}/N_{t1}. Abundance for ages 3-5 are not shown because, over the first two years, only the ages 1 and 2 have non-zero abundances.

Time	Age =1	Age =2	Total
t=0	$n_{1,0}=0$	$n_{2,0} = 0$	$N_{t0} = 0$
t=1	$n_{1,1} = \alpha_0 S/(1+\beta_0 S)$	$n_{2,1} = 0$	$N_{t1} = \alpha_0 S/(1+\beta_0 S)$
t=2	$n_{1,2} = \alpha_0 S/(1+\beta_0 S)$	$n_{2,2} = \alpha_a n_{1,1} /(1+\beta_a n_{1,1})$	$N_{t2} = \alpha_0 S/(1+\beta_0 S) + \alpha_a n_{1,1} /(1+\beta_a n_{1,1})$

Calculations are based on the assumption that all populations outside the region of extinction are at equilibrium: this is reasonable because we run the model for 200 years previous to extinction in order to achieve equilibrium in all populations: under such assumption, $n_{1,1} = n_{1,2}$.

The rate of increase is defined as $R = N_{t2}/N_{t1}$ and is given by:

$$R = \frac{\frac{\alpha_0 S}{(1+\beta_0 \cdot S)} + \frac{\alpha_a n_{11}}{(1+\beta_a \cdot n_{11})}}{\frac{\alpha_0 S}{(1+\beta_0 \cdot S)}} = 1 + \frac{\frac{\alpha_a n_{11}}{(1+\beta_a \cdot n_{11})}}{\frac{\alpha_0 S}{(1+\beta_0 \cdot S)}} = 1 + \frac{\alpha_a n_{11}(1+\beta_0 \cdot S)}{\alpha_0 S\,(1+\beta_a \cdot n_{11})},$$

with S given by eq (S1). By substituting $n_{1,1}$ (first in the numerator and then in the denominator) we get:

$$R = 1 + \frac{\alpha_a \alpha_0 S(1+\beta_0 \cdot S)}{\alpha_0 S\,(1+\beta_a \cdot n_{11})(1+\beta_0 \cdot S)} = 1 + \frac{\alpha_a}{(1+\beta_a \cdot \frac{\alpha_0 S}{(1+\beta_0 \cdot S)})}$$

Under the conditions of our model, we have $\alpha_0 = \alpha_a = 1$, $\beta_0 = \beta_a = \beta$, we obtain:

$$R = 1 + \frac{1}{(1+\frac{\beta S}{(1+\beta S)})} = 1 + \frac{(1+\beta S)}{(1+2\beta S)}$$

When the density-dependence parameter is small the population size tends to duplicate between year 1 and 2 (Fig. S4: $R \rightarrow 2$ as $\beta \rightarrow 0$); as the density-dependent parameter increases the rate of increase approaches 1.5. The population also tent to duplicates at low values of ω (either low fecundity or high larval mortality) and under low larval connectivity (low $l_{j \rightarrow p}$) which influences the value of subsidy (S). Because $T_{R=2}$ = 1-2 years for most of the combination of predictors we concluded that T_{50} as a way to study recovery times in response to extinction.

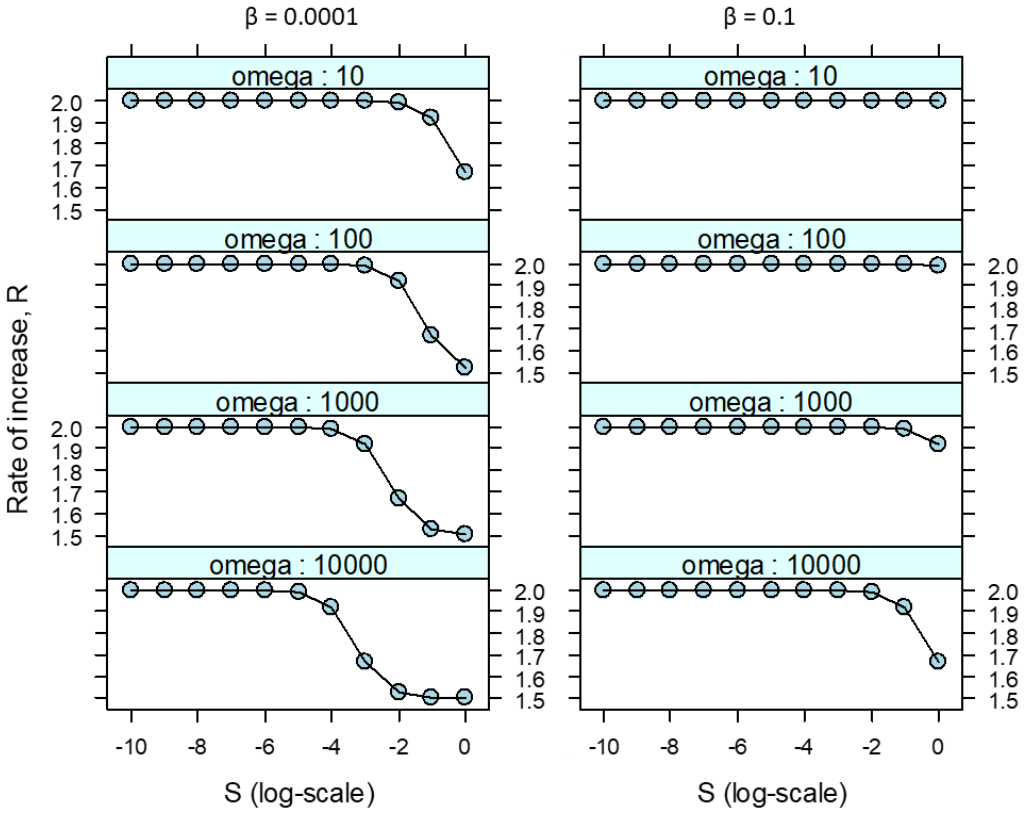

Figure S4. Changes in rate of increase during the first two years after extinction in response to subsidy (S), the density dependent coefficient (β) and ω (the product of fecundity and survival).

S3. Statistical methods and outputs

3.1 Effects of connectivity to populations outside the region of extinction

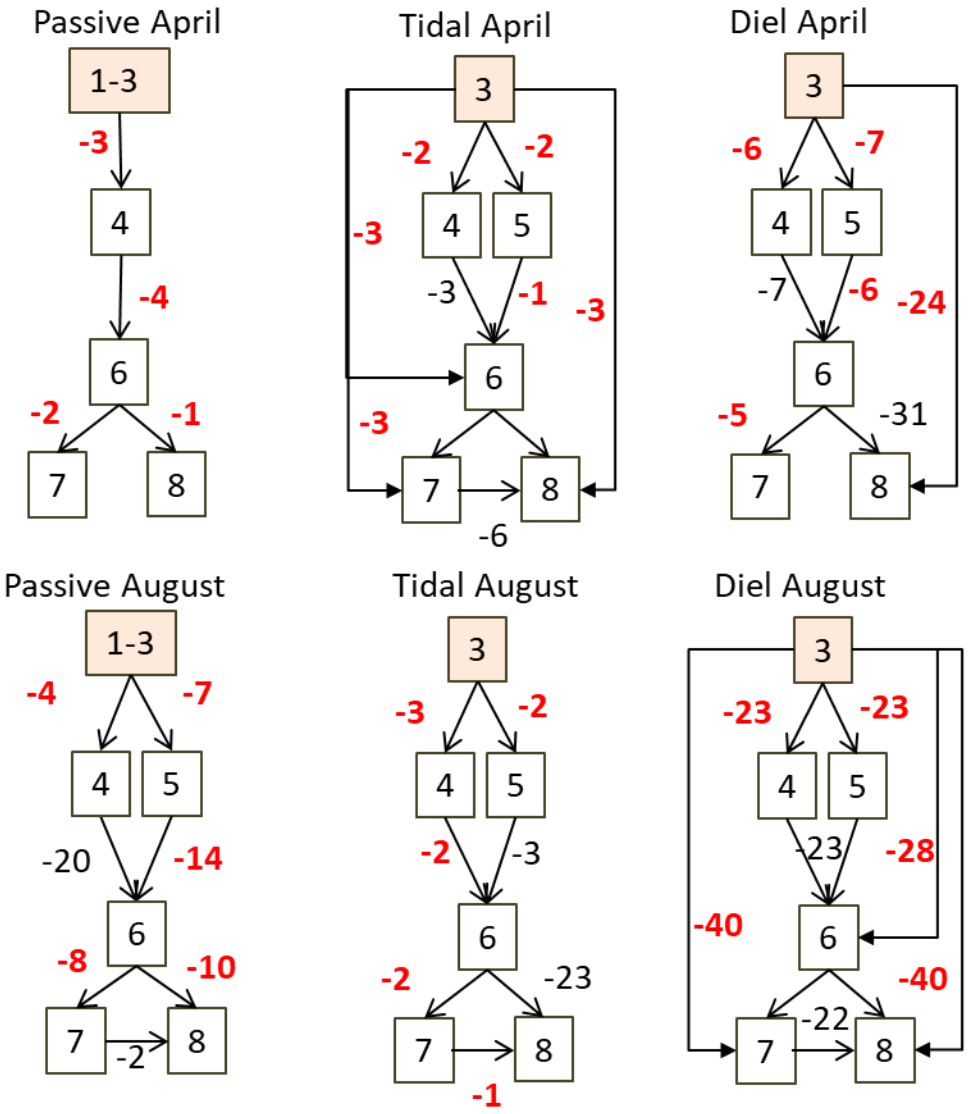

Figure S4. Summary of topology of the sub-network of Cardigan (populations 4-8) for both times of larval release (April, August) and the three larval strategies; populations are represented with numbered squares connected by arrows; the populations in grey squares are the source populations, outside the region of extinction. The topologies depend only on the larval retention (not shown) and connectivity coefficients. The larval connectivity coefficients are shown as numbers associated to arrows giving the order of magnitude (e.g. -3 corresponds to a connectivity of the order 10^{-3}). Numbers highlighted in red were used to calculate *CM*.

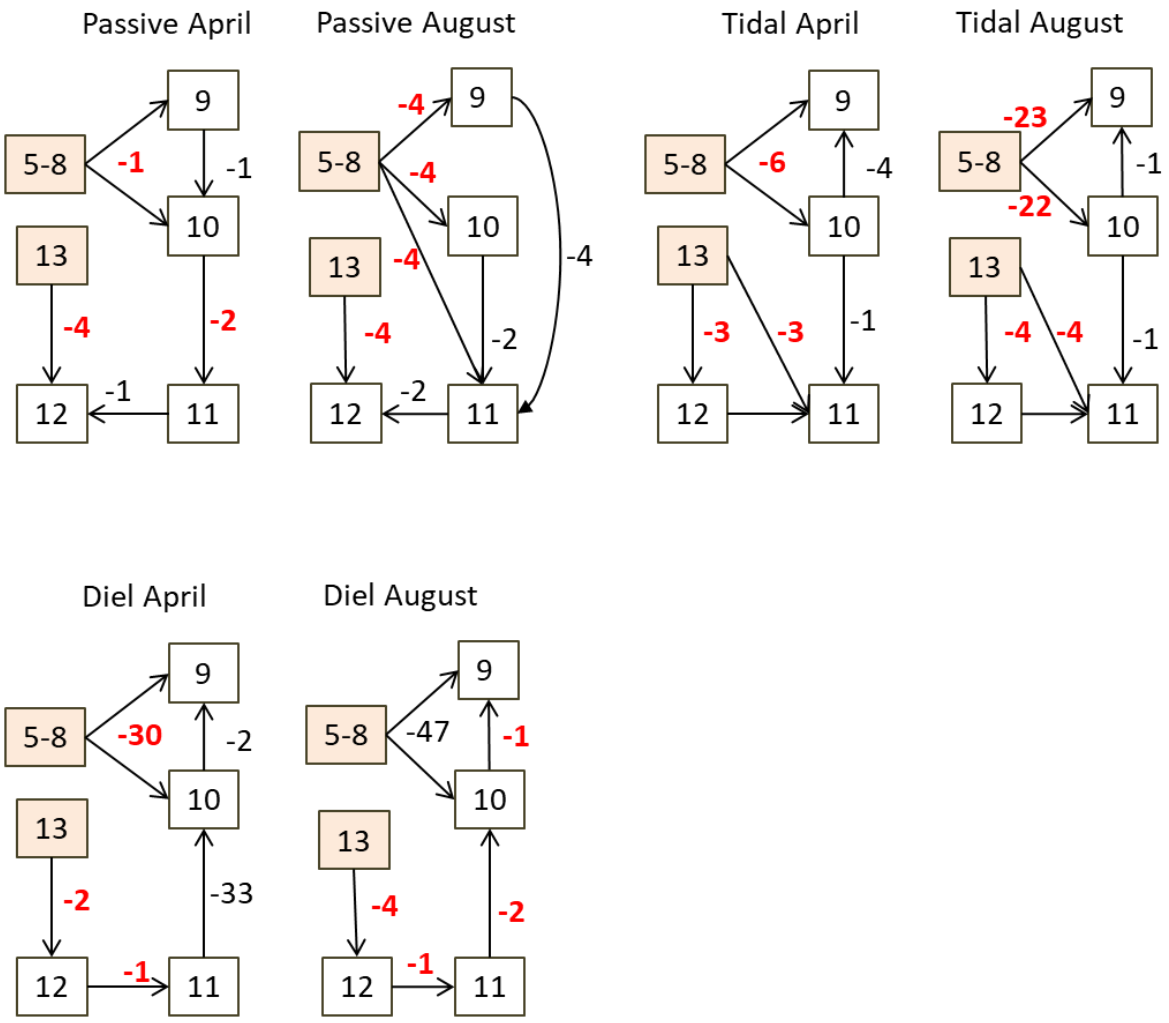

Figure S5. Summary of topology of the sub-network of Anglesey (populations 9-12) for both times of larval release (April, August) and the larval strategies; populations are represented with numbered squares connected by arrows; the populations in grey squares are the source populations, outside the region of extinction. The topologies depend on the larval retention (not shown) and connectivity coefficients. The larval connectivity coefficients are shown as numbers associated to arrows giving the order of magnitude (e.g. -1 corresponds to a connectivity of the order 10^{-1}). Numbers highlighted in red were used to calculate *CM*.

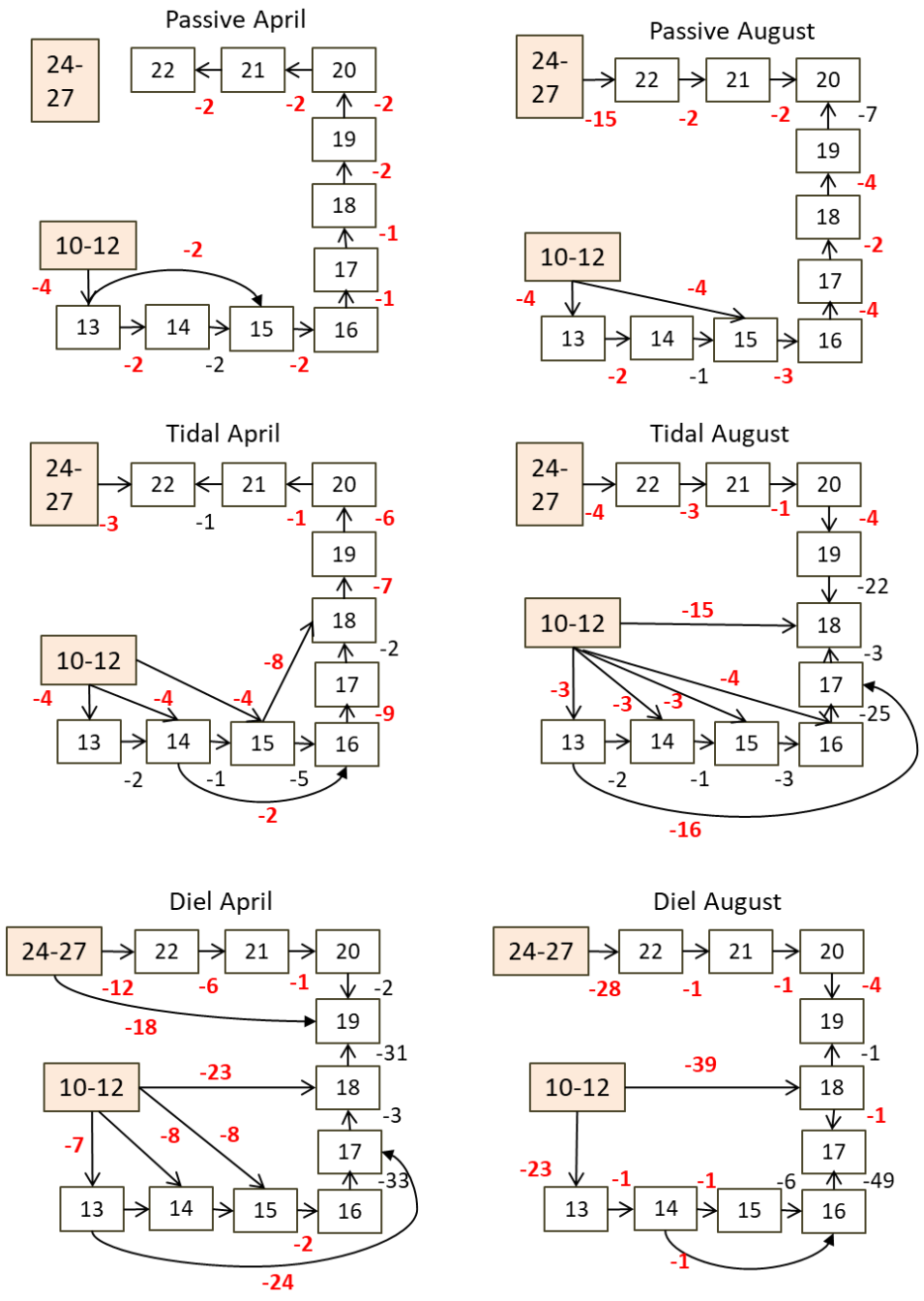

Figure S6. Summary of topology of the sub-network of Liverpool Bay (populations 13-22) for both times of larval release (April, August) and the larval strategies; populations are represented with numbered squares connected by arrows; the populations in grey squares are the source populations, outside the region of extinction. The topologies depend on the larval retention (not shown) and connectivity coefficients. The larval connectivity coefficients are shown as numbers associated to arrows giving the order of magnitude (e.g. -2 correspond to a connectivity of the order 10^{-2}). Numbers highlighted in red were used to calculate *CM*.

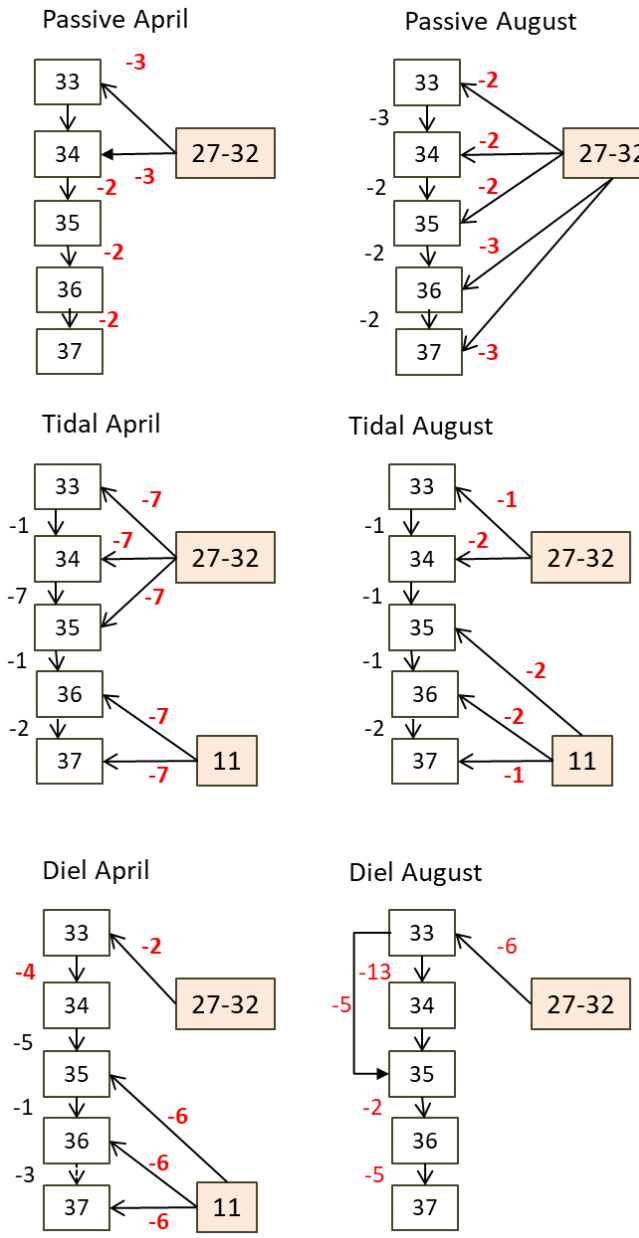

1205

1206 Figure S7. Summary of topology of the sub-network of west Irish coast for both times of larval
1207 release (April, August) and the larval strategies; populations are represented with numbered
1208 squares connected by arrows; the populations in grey squares are the source populations, outside
1209 the region of extinction. The topologies depend only on the larval retention (not shown) and
1210 connectivity coefficients. The larval connectivity coefficients are shown as numbers associated to
1211 arrows giving the order of magnitude (e.g. -3 corresponds to a connectivity of the order 10^{-3}).
1212 Numbers highlighted in red were used to calculate *CM*.

1213

1214

S4: Model output for all tested scenarios

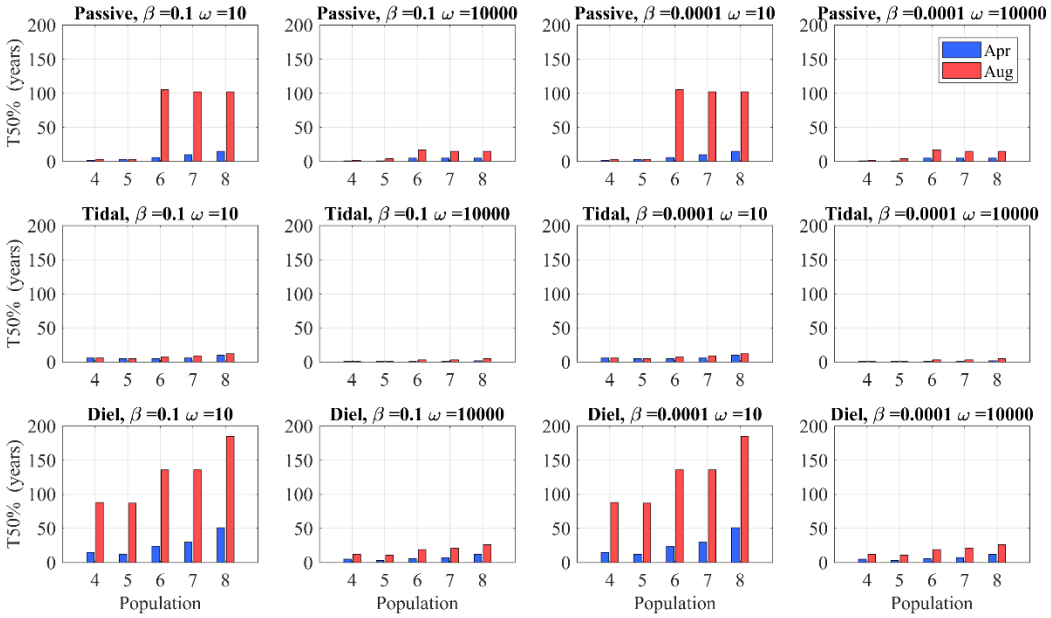

Figure S8: Cardigan Bay. Predictions of recovery times (T50%: time required to reach 50% of the numbers reached in year 400) for scenarios with combinations of larval strategies, time of larval release (bars) the density-dependent coefficient (β) and the term ω.

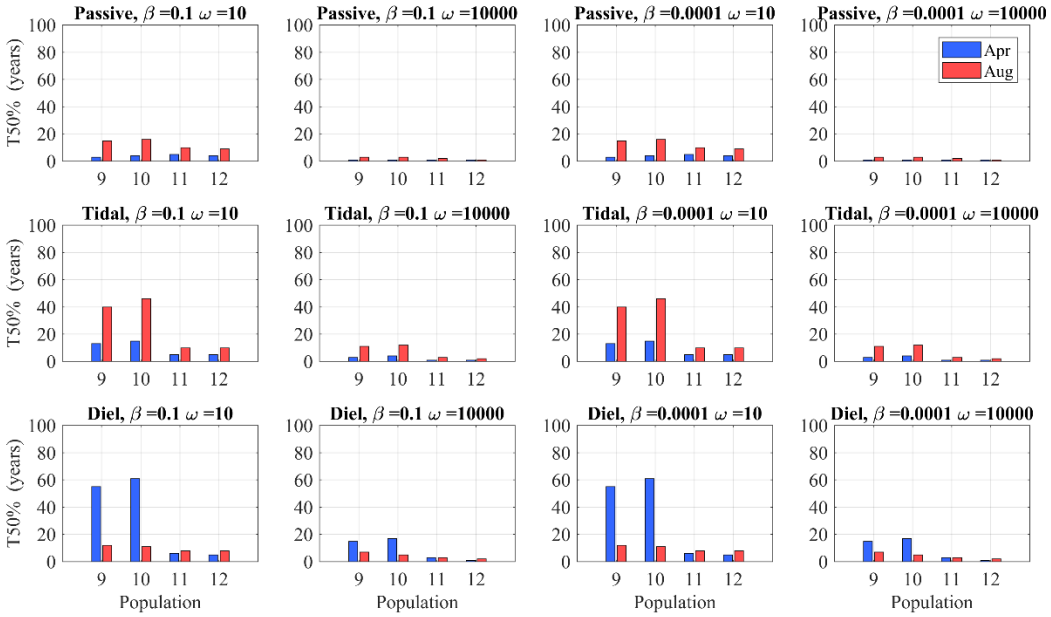

Figure S9. Anglesey. Predictions of recovery times (T50%: time required to reach 50% of the numbers reached in year 400) for scenarios with combinations of larval strategies, time of larval release (bars) the density-dependent coefficient (β) and the term ω.

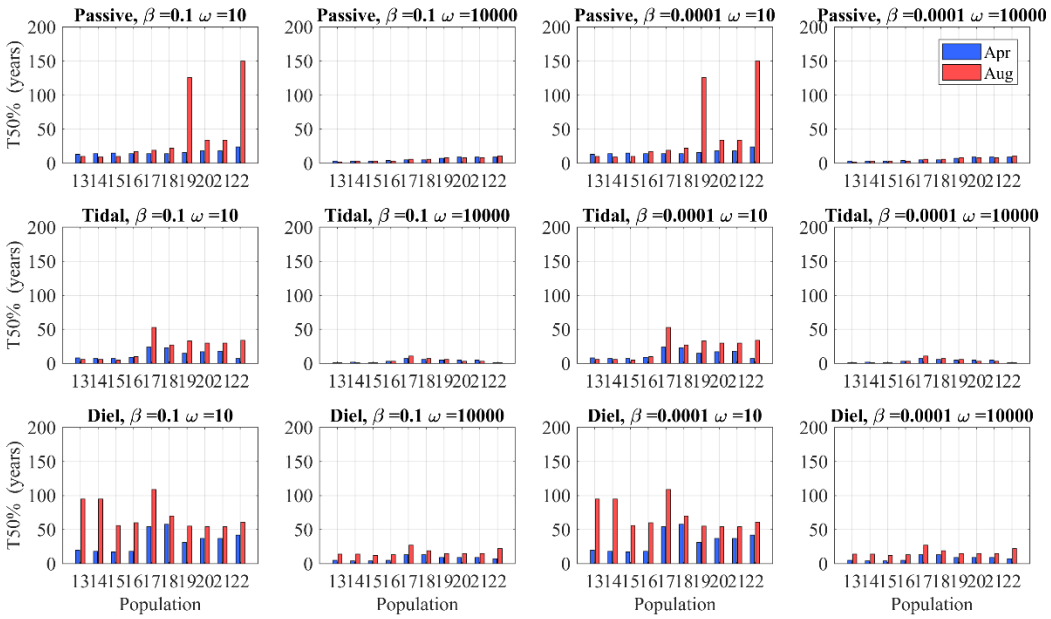

Figure S10: Liverpool Bay. Predictions of recovery times (T50%: time required to reach 50% of the numbers reached in year 400) for scenarios with combinations of larval strategies, time of larval release (bars) the density-dependent coefficient (β) and the term ω.

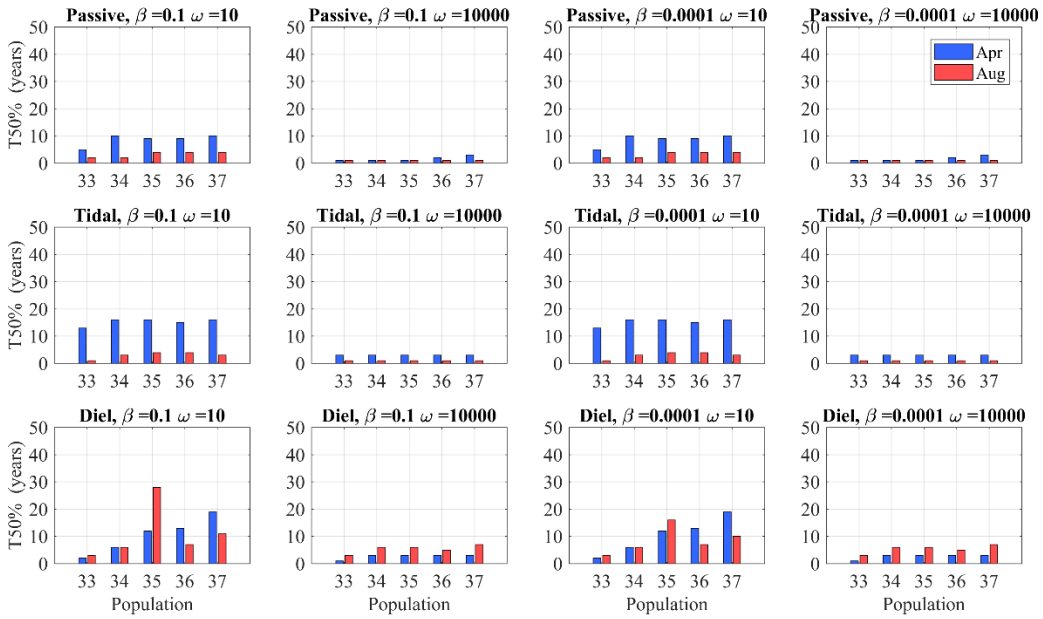

Figure S11. West Irish Coast. Predictions of recovery times (T50%: time required to reach 50% of the numbers reached in year 400) for scenarios with combinations of larval strategies, time of larval release (bars) the density-dependent coefficient (β) and the term ω.

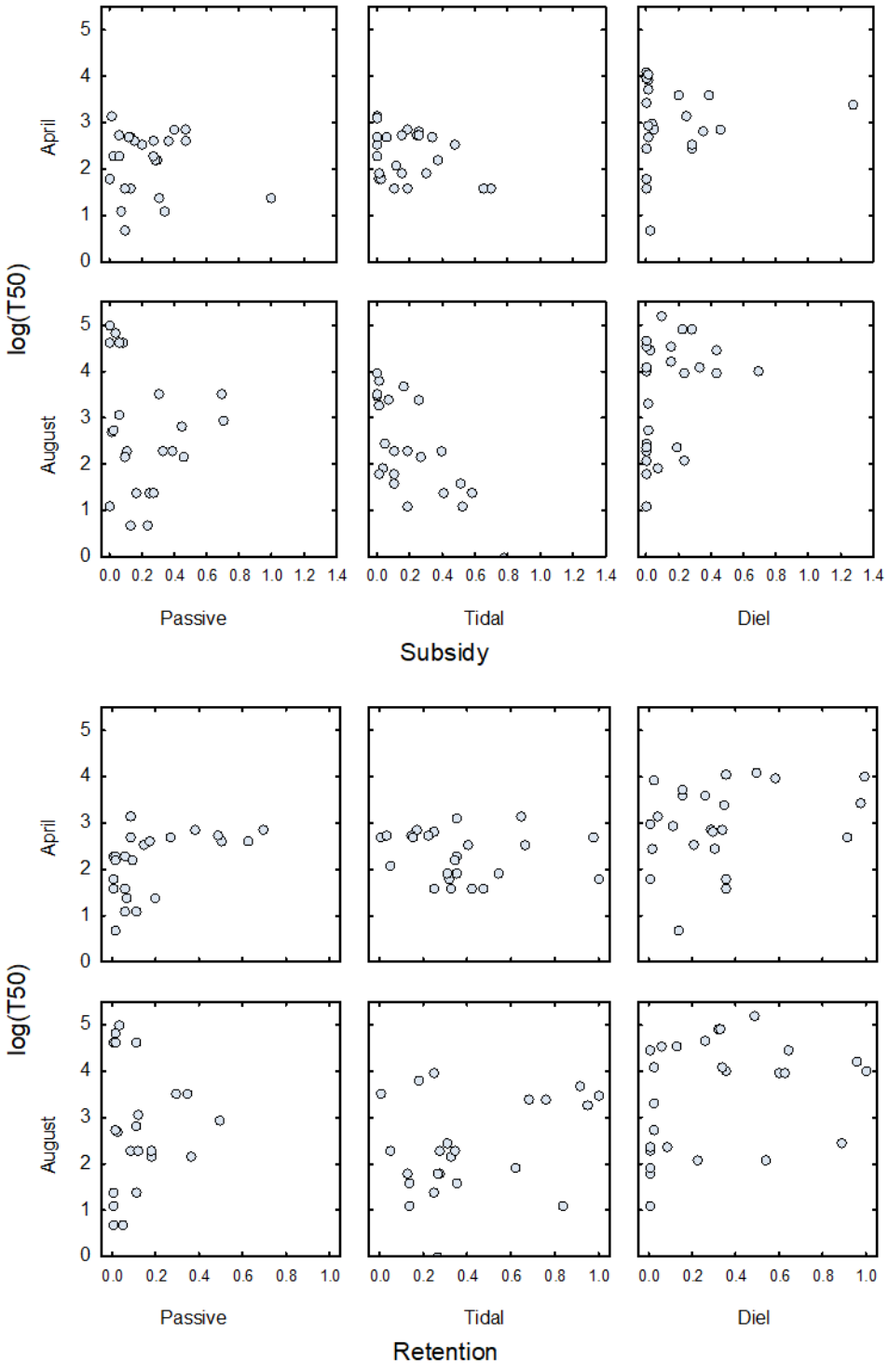

Figure S12. Scatterplots showing relationships between recovery time (log-transformed) vs subsidy (Top panels) and retention (bottom panels) for ω = 10, and for combinations of larval strategy and month of release.

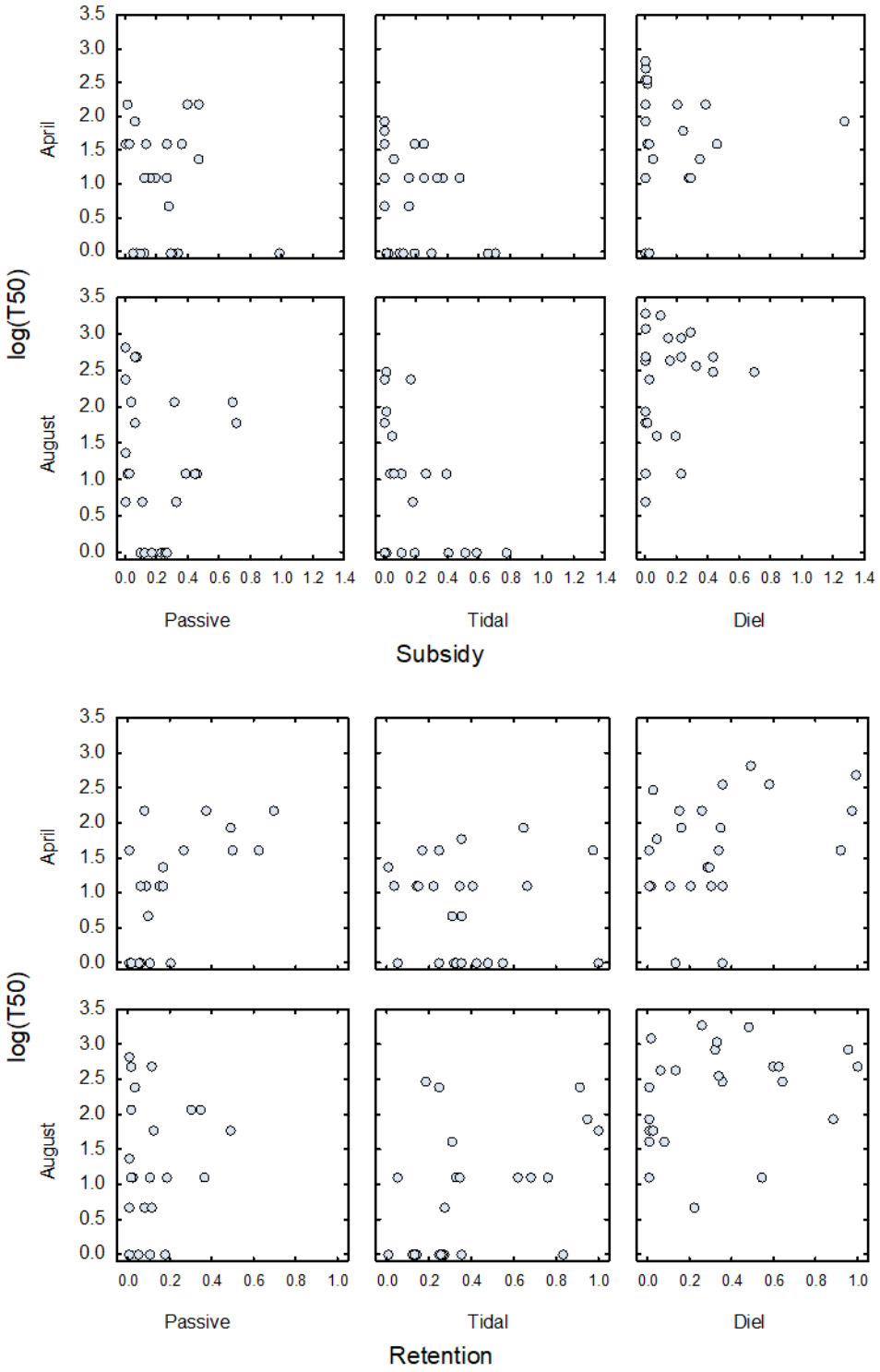

Figure S13. Scatterplots showing relationships between recovery time (log-transformed) vs subsidy (top panels) and retention (bottom panels) for $\omega = 10^4$, and for combinations of larval strategy and month of release.

1257

1258